

AD-A174 661

DAMAGE MODELS FOR DELAMINATION AND TRANSVERSE FRACTURE
IN FIBROUS COMPOST (U) TEXAS A AND M UNIV COLLEGE
STATION MECHANICS AND MATERIALS CE

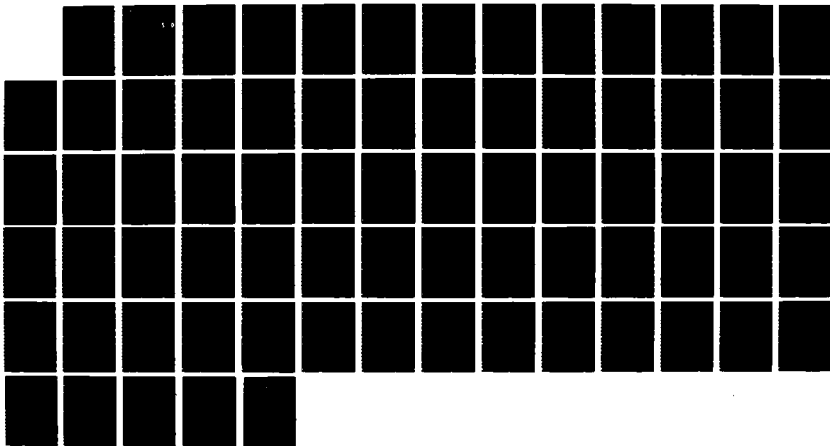
1/1

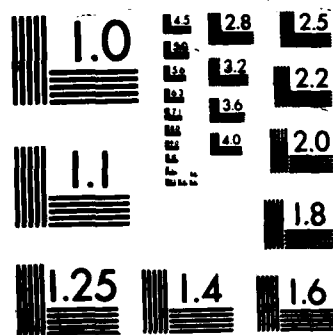
UNCLASSIFIED

R A SCHAPERY ET AL MAR 86 MM-5034-86-8

F/G 11/5

NL

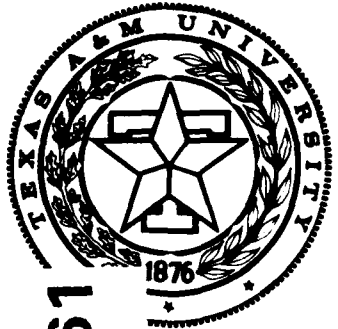




XEROCOPY RESOLUTION TEST CHART

2

Mechanics and Materials Center
TEXAS A&M UNIVERSITY
College Station, Texas



AD-A174 661

AFOSR-TR. 86-1078

DTIC
ELECTE
DEC 02 1986
S D

DAMAGE MODELS FOR DELAMINATION
AND TRANSVERSE FRACTURE

ANNUAL TECHNICAL REPORT

Approved for public release;
distribution unlimited.

R.A. SCHAPERY
M.J. LAMBORN
R.D. TONDA

AIR FORCE OFFICE OF SCIENTIFIC RESEARCH (AFSC)
NOTICE OF SUBMITTAL TO DTIC
This technical report has been reviewed and is
approved for public release IAW AFR 190-12.
Distribution is unlimited.
MATTHEW J. KEEPER
Chief, Technical Information Division

AIR FORCE OFFICE OF SCIENTIFIC RESEARCH
OFFICE OF AEROSPACE RESEARCH
UNITED STATES AIR FORCE
GRANT No. AFOSR-84-0068

OTIC FILE COPY

MM 5034-86-8

MARCH 1986

86 11 25 382

A174661

REPORT DOCUMENTATION PAGE

1a. REPORT SECURITY CLASSIFICATION unclassified			1b. RESTRICTIVE MARKINGS			
2a. SECURITY CLASSIFICATION AUTHORITY			3. DISTRIBUTION/AVAILABILITY OF REPORT Approved for public release, distribution unlimited			
2b. DECLASSIFICATION/DOWNGRADING SCHEDULE			4. PERFORMING ORGANIZATION REPORT NUMBER(S) MM-5034-86-8			
5. MONITORING ORGANIZATION REPORT NUMBER(S) AFOSR-TR- 86-1078			6a. NAME OF PERFORMING ORGANIZATION Mechanics and Materials Center Texas A&M University			
6b. ADDRESS (City, State and ZIP Code) College Station, TX 77843			6b. OFFICE SYMBOL (If applicable)			
7a. NAME OF MONITORING ORGANIZATION AFOSR/NA			7b. ADDRESS (City, State and ZIP Code) Building 410 Bolling AFB, DC 20332-6448			
8a. NAME OF FUNDING/SPONSORING ORGANIZATION AFOSR			8b. OFFICE SYMBOL (If applicable) N A			
9. PROCUREMENT INSTRUMENT IDENTIFICATION NUMBER AFOSR-84-0068			9c. ADDRESS (City, State and ZIP Code) Building 410 Bolling AFB, DC 20332-6448			
10. SOURCE OF FUNDING NOS.			11. TITLE (Include Security Classification) Damage Models for Delamination and Transverse Fracture in Fibrous Composites			
PROGRAM ELEMENT NO. 61102F			PROJECT NO. 2302		TASK NO. B2	
12. PERSONAL AUTHOR(S) R.A. Schapery, M.J. Lamborn, R.D. Tonda			13a. TYPE OF REPORT Annual			
13b. TIME COVERED FROM 2/15/85 TO 2/14/86			14. DATE OF REPORT (Yr., Mo., Day) March, 1986		15. PAGE COUNT 10 + Appendix	
16. SUPPLEMENTARY NOTATION						
17. COSATI CODES			18. SUBJECT TERMS (Continue on reverse if necessary and identify by block number)			
FIELD	GROUP	SUB. GR.	Composites			
			Fracture of Composites			
			Damage			
			Fiber-Reinforced Plastic			
			Delamination			
19. ABSTRACT (Continue on reverse if necessary and identify by block number) Theoretical and experimental work on the deformation and fracture of fibrous composites with distributed damage is described. Emphasis is on establishing the existence of potentials analogous to strain energy and on using these so-called work potentials in fracture studies. The difference between changing damage and constant damage processes is accounted for by using multivalued work potentials. It was shown previously that these potentials lead to a path independent J integral for characterizing fracture. A recent study is described in this report in which the J integral is used to determine fracture energy for delamination in double-cantilevered beam specimens with a large percentage of off-axis fibers; the results are compared with fracture energies found by standard methods (which do not account for effects of distributed damage). Discussed next are investigations of flat rectangular bar specimens and thin-walled tubes under axial and torsional loading. The limited amount of experimental data presently available on angle-ply laminates confirms the existence of a potential even when there are large increases in microcracking. The Appendix contains copies of technical reports prepared during the project year and the abstract of a recently completed Ph.D. dissertation.						
20. DISTRIBUTION/AVAILABILITY OF ABSTRACT UNCLASSIFIED/UNLIMITED <input checked="" type="checkbox"/> SAME AS RPT. <input type="checkbox"/> DTIC USERS <input type="checkbox"/>			21. ABSTRACT SECURITY CLASSIFICATION unclassified			
22a. NAME OF RESPONSIBLE INDIVIDUAL Dr. N.J. Pagano Dr. Salkind			22b. TELEPHONE NUMBER (Include Area Code) (202) 767-4937		22c. OFFICE SYMBOL NA	

TABLE OF CONTENTS

1. RESEARCH OBJECTIVES 1

2. STATUS OF THE RESEARCH 1

 2.1 Overview 1

 2.2 Studies of Flat Laminates Under Axial and
 Torsional Loading 3

 2.3 Studies of Tubes Under Axial and Torsional Loading 5

3. LIST OF AFOSR SPONSORED PUBLICATIONS 8

4. PROFESSIONAL PERSONNEL INFORMATION 8

 4.1 List of Professional Personnel 8

 4.2 Spoken Papers (Principal Investigator's
 Activities)..... 9

5. APPENDIX 10

Accession For	
NTIS	<input checked="" type="checkbox"/>
CRA&I	<input type="checkbox"/>
DTIC	<input type="checkbox"/>
TAB	<input type="checkbox"/>
Unannounced Justification	
By	
Distribution /	
Availability Codes	
Dist	Avail and/or Special
A-1	



1. RESEARCH OBJECTIVES

The overall objective of the research is to develop and verify mathematical models of delamination and transverse fracture which account for local (crack tip) and global damage distributions. One specific objective is to demonstrate theoretically and experimentally that "work potentials" (which are analogous to strain energy) exist for composites with constant and changing damage and with viscoelastic behavior. The second objective is to develop and verify methods of analysis for predicting crack growth in elastic and viscoelastic composites with distributed damage; whenever they are justified, work potentials will be used to characterize material behavior in order to simplify fracture analysis.

2. STATUS OF THE RESEARCH

2.1 Overview

Methods of deformation and fracture characterization and prediction are simplified when strain energy-like potentials based on mechanical work can be used, as described in the first paper in the Appendix, "Deformation and Fracture Characterization of Inelastic Composite Materials Using Potentials". With these so-called work potentials, important theoretical and experimental methods using the J integral and energy release rate (originally developed for fracture of elastic media and fracture initiation in metals with plastic deformations) may be extended to fracture initiation and crack propagation in monolithic and composite materials.

The second paper in the Appendix, "Delamination Analysis of Composites with Distributed Damage Using a J Integral", describes an experimental study made during the project year on delamination of composites with

multiple fiber orientations. The J integral was used to determine the fracture energy. Considering the theoretical basis for this method (which is given in the first paper in the Appendix) and the consistency of fracture energies obtained, it is believed the J integral method is more appropriate for determining fracture energy than other existing techniques when there are significant effects of distributed damage on specimen deformations. A new Ph.D. student, Mr. Douglas Goetz, (who is supported jointly by the subject grant and Dr. W.L. Bradley's AFOSR grant) plans to continue the work on the J integral through additional investigations of delamination. Effects of multiple loads or deformation states, such as combined bending and stretching or compression, as well as various layups (including different thicknesses) and specimen types, will be studied to determine, in part, whether or not the J-determined fracture energy is sensitive to geometry and loading conditions.

Another Ph.D. student, Mr. Mark Lamborn, is studying flat angle-ply bars under combined axial and torsional loading. Some of his early work is discussed in the first paper in the Appendix. This investigation is concerned primarily with (i) the determination of work potentials for specimens with significant amounts of distributed damage and (ii) use of the J integral to characterize and predict edge delamination when distributed damage and the mode III (antiplane) component of energy release rate are relatively large. He summarizes the status of this effort in Section 2.2. Studies to-date indicate that a work potential exists; but much more effort is needed to establish its range of existence and to obtain a detailed characterization.

A third graduate student, Richard Tonda, describes in Section 2.3 his work on determining work potentials for a graphite/epoxy composite using

circular tubes and flat bars. The computer, computer programs, and reduced data were all lost in a fire on December 31, 1984. This study was discontinued for a year and thus was only recently restarted.

Graduate student Randy Weatherby completed a Ph.D. dissertation in January 1986. It describes the development and application of a new finite element model for analyzing crack growth in materials which are characterized by work potentials. It is believed that both the use of the crack tip "failure zone" in a finite element model and the study of path independence of the J integral with macro-crack propagation and distributed micro-damage are new. The abstract of the dissertation is included at the end of the Appendix.

2.2 Studies of Flat Laminates Under Axial and Torsional Loading

Various layups were tested under the conditions of combined axial and torsional loads to obtain some insight on work potentials and on which layups would result in significant coupling effect of rotation and axial deformation on loads. The tests were performed for conditions of proportional and non-proportional straining. The axial displacement and rotation were controlled during each test. All test specimens were rectangular bars consisting of 24 plies, and either balanced angle-ply or balanced symmetric laminates. Test specimens were relatively long bars of various lengths and widths. The test results indicate that of the laminates tested, a $[\pm 20_12]_S$ with a length to width ratio of 6 displayed the most coupling. All test specimens failed at significantly lower torque levels than the torque capacity of the load cell. A new load cell which will be more sensitive to low torque levels has been ordered and shipment is expected in the early summer.

A computer program has been developed which takes the measurements from a series of proportional straining tests and checks for the existence of a potential. A series of data was generated using a nonlinear material model for which the analytical expression for the potential was known. The computer program showed the existence of this potential thus verifying the procedure. The program has been used to study proportional straining tests to determine the type and number of tests required to verify the existence of a potential. These studies indicated that several of the specimens in a series of tests should be tested at relatively low ratios of axial displacement to rotation. Work is underway to modify this program to permit checking for the existence of a potential between specific levels of the axial displacement and rotation. Checking for the existence of a potential in this manner will allow fewer experimental tests.

A MTS tension-torsion testing machine was used to perform all tests. It was determined that the axial displacement as measured by this machine may be in error in some cases due to displacements in the grip mechanism. To determine the magnitude of this error aluminum test specimens, corresponding to ASTM standard tensile specimens, were mounted with strain gages. These specimens were tested under combined axial and torsional loads in a series of proportional straining tests. The axial displacement was determined from measurements by strain gages, a LVDT, and the crosshead movement. Good agreement was found between the axial displacements measured by the strain gages and the LVDT. These measurements were different than those from crosshead movement. The LVDT measurements were used in calculations to determine the existence of a potential with elastic-plastic deformation of aluminum test specimens; the calculations showed that a potential did exist, as expected. The LVDT will be used in

future tests to measure the axial displacement.

2.3 Studies of Tubes Under Axial and Torsional Loading

The 1985 annual report documented progress in this area of the research effort and indicated that the effort was brought to a stand-still as a result of a fire which destroyed the Texas A&M facility being used to store, process and analyze these data. Funding and legislative considerations led to a delay in the acquisition and installation of the necessary hardware until early October, 1985. Work was recently initiated to restore the software and data which was previously lost.

Our earlier analysis indicated that it was useful to conduct an experimental and analytical study of angle-ply laminates under multiaxial loading in order to verify the existence and use of a work potential for modelling realistic amounts of distributed damage. This laminate/loading condition combination undergoes significantly more damage prior to global fracture than the unidirectional off-axis tensile samples tested earlier, and therefore provides data which enable a more critical evaluation of the work potential theory. The unidirectional studies provided baseline elastic and viscoelastic property data in the absence of the residual stresses which exist in angle-ply laminates, and thus can be used to predict baseline angle-ply response with no significant damage.

Prior to the fire mentioned earlier, the decision was made to conduct cylindrical tube tests under combined axial and torsional loading. This test technique offered two features necessary to expand on the work already completed. First, angle-ply laminates of arbitrary construction could be tested, and second this testing could be accomplished under a truly independent, bi-axial state of stress. Hercules, Inc., of Magna, Utah, provided four (4) cylindrical specimens of angle-ply laminates constructed

from the same material and production line as that used for the off-axis tests conducted earlier. These four tubes were carefully constructed and layed-up by hand, and as such represent high-quality structures to be used in the final phase of testing. This set of specimens consists of two $[\pm 30]_{2S}$ and two $[\pm 60]_{2S}$ tubes, all 2 inch dia x 20 inches long. Because of the considerable value of these tubes, and to better understand and characterize the phenomena being observed, we obtained and validated a finite-element routine which allowed for careful and optimized use of the four tubes available. The NISA program for the HP 1000 computer was made available at very low cost, and since it was highly capable in the area of composites, was chosen for this analysis. The fire mentioned earlier put a complete halt to this process as well.

A new copy of NISA was obtained in late December of 1985 and was installed and checked out in January of 1986. Work is now underway to validate the models of both tube and off-axis specimens. Preliminary analysis with NISA and our prior experience with composites testing has indicated a need for more test samples. Due to the high cost and long lead time for preparation and acquisition of additional tubes like those already supplied, discussions have continued with Hercules to have a number of additional specimens fabricated. Those specimens will be eight-ply, 2 inch dia X 20 inch long tubes like the more costly hand layed-up tubes already on hand. Instead of hand lay-up however, these tubes will be rolled from prepreg tape in an assembly line fashion. It is anticipated that specimen quality and consistency will be more variable in comparison to the hand lay-up technique, but a number of these tubes will be used to develop experimental and data reduction techniques and to provide baseline laminate performance and behavior. A quotation has been requested from Hercules for 18 tubes total: 6 $[\pm 30]_{2S}$, 6 $[\pm 60]_{2S}$, and 6 $[\pm 20]_{2S}$. We anticipate placing

an order for these items shortly so that the tubes will be delivered in April.

Current efforts are concentrating on NISA simulations which examine the effect of grip technique on specimen response and on developing a test matrix to maximize the efficient use of the number of specimens we hope to have available. If all proceeds according to plan, tube testing will start in late April.

3. LIST OF AFOSR SPONSORED PUBLICATIONS

R.A. Schapery, "Deformation and Fracture Characterization of Inelastic Composite Materials Using Potentials". To be published in Polymer Engineering and Science.

R.A. Schapery, W.M. Jordan, and D.P. Goetz, "Delamination Analysis of Composites with Distributed Damage Using a J Integral". To be published in the proceedings of the International Symposium on Composite Materials and Structures, Beijing, June 1986.

J.R. Weatherby, "Finite Element Analysis of Crack Growth in Inelastic Media". Ph.D. dissertation, Texas A&M Univ., completed and approved Jan. 1986. Papers based on this dissertation will be prepared during the year.

4. PROFESSIONAL PERSONNEL INFORMATION

4.1 List of Professional Personnel

1. Richard Schapery, Principal Investigator
2. Douglas Goetz, Graduate Research Assistant
3. Mark Lamborn, Graduate Research Assistant
4. Richard Tonda, Graduate Research Assistant
5. Randy Weatherby, Graduate Research Assistant. (Ph.D. requirements were completed Jan. 1986)
6. Bob Harbert, Assistant Research Engineer, (Laboratory Staff Member)
7. Carl Fredericksen, Electronics Technician, (Laboratory Staff Member)

4.2 Spoken Papers (Principal Investigator's Activities)

1. "Fracture Analysis of Nonlinear Viscoelastic Materials", Mechanics Seminar, Tel-Aviv Univ., Tel-Aviv, Feb. 1985.
2. "Fracture Analysis of Composite Materials", Composites Group at Israel Aircraft Industries, Tel-Aviv, Feb. 1985.
3. "Recent Developments on Damage Growth and Fracture of Composite Materials", Plenary lecture at Israel Aeronautics Conference, Haifa, March 1985.
4. "Deformation and Fracture Characterization of Inelastic Nonlinear Materials Using Potentials", Mechanics Seminar, Univ. of Texas, Austin, April 1985.
5. "A Micromechanics Model for Nonlinear Viscoelastic Behavior of Particle-Reinforced Rubber with Distributed Damage", Int. Union of Theoretical and Applied Mechanics Conf. on Fatigue and Damage, Technion, Haifa, July 1985.
6. "Deformation and Fracture Characterization of Inelastic Composite Materials Using Potentials", International Symposium on Nonlinear Deformation, Fracture and Fatigue of Polymeric Materials, National Meeting of the American Chemical Society, Chicago, Sept. 1985.

5. APPENDIX

Publications on AFOSR Project:

1. "Deformation and Fracture Characterization of Inelastic Composite Materials Using Potentials"
2. "Delamination Analysis of Composites with Distributed Damage using a J Integral"
3. "Finite Element Analysis of Crack Growth in Inelastic Media" (Abstract)

DEFORMATION AND FRACTURE CHARACTERIZATION
OF INELASTIC COMPOSITE MATERIALS
USING POTENTIALS*

R. A. Schapery

Mechanics and Materials Center

Department of Civil Engineering

Texas A&M University, College Station, Texas 77843

ABSTRACT

An approach using strain energy-like potentials to characterize deformation and fracture of inelastic, nonlinear composite materials is described. The inelasticity may be due to various causes, including microcracking, microslipping, and rate processes responsible for fading memory (viscoelasticity). The concept of work potentials is introduced first, and then arguments are given for their existence for inelastic materials. Emphasis in the paper is on elastic composite materials with changing or constant states of distributed damage. Experimental results on polymeric composites are subsequently presented to illustrate this approach to deformation and fracture characterization. Finally, extension to viscoelastic behavior is discussed.

*Presented at the International Symposium on Non-Linear Deformation, Fracture and Fatigue of Polymeric Materials, National Meeting of the American Chemical Society, Chicago, September 1985.

1. Introduction

Many important results on the deformation and fracture of linear and nonlinear elastic materials have been obtained by using strain energy functions or potentials to characterize material response. The thermodynamics of reversible processes provides theoretical support for the existence of these potentials and identifies them as free energy and internal energy for isothermal and adiabatic processes, respectively (e.g., Fung (1)). Besides serving as the basis for powerful methods of exact and approximate structural analysis, strain energy functions have been used in the prediction of effective or average constitutive properties (or their upper and lower bounds) of linear multiphase media in terms of properties and geometry of the phases, as reviewed by Hashin (2). Included in the many publications in this area are studies of the influence of small distributed cracks on the effective stress-strain behavior of monolithic and composite materials, like those described by Hashin (2) and Kachanov (3).

Methods of characterization and analysis using local and global strain energy-like potentials for certain inelastic materials, namely viscous, plastic, and elementary types of viscoelastic bodies, have been discussed in an early work by Hill (4). Constitutive equations normally employed for linear and nonlinear viscous bodies are fully analogous to those for elastic media, in which strain rate replaces strain (4). For the linear viscous and viscoelastic cases one may use irreversible thermodynamics (5) or special types of material symmetry, i.e. cubic and isotropic (6), to argue for the existence of strain energy-like constitutive potentials in terms of physical or Laplace-transformed variables (7). While experimental data on multiaxial nonlinear viscous behavior of metals (corresponding to the secondary creep

stage) may be characterized analytically through a potential, a general theoretical basis for this constitutive potential does not appear to exist in either irreversible thermodynamics or in models of micromechanisms; Rice (8) concluded that there is no sufficiently general physical model of slip which is capable of providing a firm basis for the existence of a creep potential. Duva and Hutchinson (9) give a good illustration on the use of potentials to construct approximate effective constitutive equations of nonlinear viscous composites; in this analysis the composite is a homogeneous, isotropic, incompressible, power-law nonlinear material with a given dilute concentration and size of spherical voids or penny-shaped cracks.

In using a potential to characterize constitutive equations it is often sufficient to account explicitly for only a dependence of the potential on the stress or strain (or strain rate) tensor. If the effect of different temperatures or other parameters, such as microvoid or microcrack fractions and sizes, are of interest, then one would of course have to consider how these quantities affect the constitutive potential. An example of such a potential for an elastic material with damage is the volume-averaged strain energy density of a material specimen, $W(e_{ij}, D_k)$, where e_{ij} are components of a suitably defined volume-averaged strain tensor and D_k represents a set of "damage" parameters which defines the current damage state (e.g. microcrack sizes). The stresses for this material are then obtained by differentiating W with D_k fixed,

$$s_{ij} = \partial W / \partial e_{ij} \quad (1)$$

In references (2), (3), and (9), the effects due to specified sizes and concentrations, D_k , of microcracks are considered. If it is further desired to characterize the effective constitutive behavior when the D_k change with

time as a result of straining, then relationships governing these changes must be determined. Suppose for discussion purposes that these relationships are known and that one may solve the equations so as to express the damage parameters D_k in terms of the instantaneous strains e_{ij} . For some cases, it may then be possible to find a strain energy-like potential $\hat{W}(e_{ij})$, say, from which the effective constitutive equations can be derived by differentiation,

$$s_{ij} = \frac{\partial \hat{W}}{\partial e_{ij}} \quad (2)$$

This constitutive potential would depend on only the instantaneous strains but yet account for changing damage. If such a potential could be found, it would be like that used to characterize elasto-plastic behavior of metals by the Hencky deformation theory (10). Similarly, it would be analogous to the potential for metals discussed by Rice (8) for stationary creep; in his case the "damage" is an idealized set of internal slips which contribute to the average strain rate but do not appear explicitly in the effective stress-strain rate equations for the metal.

The present paper deals in large part with the question of whether or not potentials analogous to $\hat{W}(e_{ij})$ exist for elastic, viscous, and viscoelastic composites with changing damage (or, more generally, changing microstructure); emphasis is on elastic behavior with damage. Theory (Sections 2 and 3) and related experimental work using data on a particle-filled rubber and fiber-reinforced plastics (Sections 4-6) are discussed.

We should add that there are already many publications on the thermodynamic and micromechanistic bases for constitutive potentials for different types of inelastic materials; see, for example, Rice (8,11), Coleman and Gurtin (12), and Schapery (13-15). However, these potentials depend

explicitly on "internal" parameters which reflect the microstructure state, and are thus like $W(e_{ij}, D_k)$ in Eq. (1). They do not necessarily lead to the simplified form $\hat{W}(e_{ij})$ of particular interest here.

Strain energy potentials have been used widely in fracture mechanics (e.g., Broek (16)). For fully elastic materials, the mechanical work available at a crack tip for producing an increment of crack growth is equal to the decrease in potential energy (consisting of global strain energy and the boundary-work potential). Use of this relationship has resulted in remarkably successful investigations of fracture of rubber in its nonlinear range of behavior, which are reviewed by Lake (17), as well as fracture of linear elastic materials (16). Andrews (18) assumed a strain energy-like potential exists for rubber with hysteresis, and suggested how the hysteresis would affect crack growth. When a potential exists it is often possible to use Rice's J integral theory (19) to simplify fracture analysis. Schapery (20) recently extended the potential energy and J integral theories to elastic and viscoelastic materials with damage.

Concepts from fracture mechanics are used in Section 3 to obtain the equations needed to predict microcrack growth, and thus help provide the basis for potentials, such as $\hat{W}(e_{ij})$ in Eq. (2). Also, potentials are used in Section 6 to account for the effect of inelastic material behavior (which may be due to microcracking) on the growth of a macrocrack in the form of a delamination.

In most of this paper (Sections 2-6) it is assumed the materials are elastic when the damage is constant. In Section 7 a special representation of viscoelastic behavior proposed by Schapery (15,20) is used to extend the elastic theory with damage to linear and nonlinear viscoelasticity; viscous

behavior appears as a special case.

Finally, it should be mentioned that for lack of a better term we are using "damage" when referring to characteristics of the microstructure or fabric of a material which affect constitutive behavior but are not accounted for in elastic or fading-memory viscoelastic characterizations of continua. Furthermore, a damaging process, such as considered here, could be associated with crack growth, crack healing, dislocation creation and motion, breaking or reforming entanglement points along polymer chains in rubber, etc., and therefore may be structurally detrimental or beneficial.

2. One-Dimensional Theory

The definition of a potential for elastic materials with damage may be explicitly introduced through the uniaxial stress-strain curve in Fig. 1. Let us suppose that a previously unloaded specimen is strained monotonically until the strain is e_m . (By definition, the initial state is "undamaged".) The strain is then reduced, as shown in Fig. 1. Assuming that the bar is elastic and has constant damage during the unloading period, with instantaneous stress s^U , and using the same idealization as Gurtin and Francis (21) in which the maximum strain e_m serves to define the amount and effect of damage,

$$s^U = f(e, e_m) \quad (3)$$

On the loading curve, the maximum strain is the current strain. Hence, viewing the loading stress as a point at the upper end of an unloading curve, we may write

$$s^L = f(e, e) \quad (4)$$

The mechanical work (per unit initial volume) during loading to an arbitrary strain is

$$w^L = w^L(e) = \int_0^e s^L de' = \int_0^e f(e', e') de' \quad (5)$$

where the prime denotes a dummy variable of integration. The net work input to the sample at any time during unloading is the shaded area in Fig. 1,

$$\begin{aligned} W^U &= W^U(e, e_m) = W^L(e_m) + \int_{e_m}^e s^U de' \\ &= W^L(e_m) + \int_{e_m}^e f(e', e_m) de' \end{aligned} \quad (6)$$

Observe that during loading and unloading, respectively,

$$s^L = dW^L/de, \quad s^U = \partial W^U/\partial e \quad (7)$$

It is convenient to let W denote a continuous quantity which equals W^L during loading ($e_m = e$) and equals W^U during unloading ($e \leq e_m$). Then, we may write for both loading and unloading processes,

$$s = \partial W/\partial e \quad (8)$$

The strain energy-like quantity W is actually the net work to the material at any stage of loading or unloading, and thus it will be called a work potential. It becomes the usual strain energy density when the loading and unloading curves are identical. Obviously, a work potential W can always be constructed, given the uniaxial stress-strain behavior, Eqs. (3) and (4).

Derivatives of multidimensional equations are needed in the next section. The one-dimensional model, Eqs. (3) and (4), is useful for clarifying some of the analysis ahead of time. In particular, observe that the slope of the unloading curve is,

$$\frac{\partial s^U}{\partial e} = \frac{\partial f}{\partial e} = \frac{\partial^2 W^U}{\partial e^2} \quad (9)$$

The loading curve s^L is a function of only e . However, when using the upper

end of the unloading curve to define s^L , both arguments in $f(e, e_m)$ must be considered in computing the derivative,

$$\frac{ds^L}{de} = \frac{\partial f}{\partial e} + \frac{\partial f}{\partial e_m} \frac{\partial e_m}{\partial e} = \frac{\partial f}{\partial e} + \frac{\partial f}{\partial e_m} \quad (10)$$

where we have used the fact that $e_m = e$ on the loading curve. (The last term in Eq. (10) is the difference in slopes of the two curves at $e_m = e$.) We may rewrite Eq. (10) using Eq. (3) and the second expression in Eq. (7) to obtain

$$\frac{ds^L}{de} = \frac{\partial^2 W^U}{\partial e^2} + \frac{\partial^2 W^U}{\partial e \partial e_m} \quad (11)$$

where the derivatives of W^U are to be evaluated at $e_m = e$ after differentiation.

3. Multidimensional Theory

For characterization of multiaxial stress-strain behavior, or for other responses which depend on more than one independent input, a work potential does not necessarily exist. However, that it can be expected to exist for some realistic situations will be discussed here. For the sake of generality let us use as independent inputs the generalized displacements q_j ($j=1,2,\dots,J$). The responses are the generalized forces Q_j , which are defined in the usual way by the condition that, for each j ,

$$\delta(Wk) = Q_j \delta q_j \quad (12)$$

where $\delta(Wk)$ is the virtual work input associated with the virtual displacement δq_j . Suppose, for example, that we let each q_j represent a gradient, $\partial u_m / \partial x_n$ ($m,n=1,2,3$) of a three-dimensional displacement field, u_m , and let $\delta(Wk)$ be virtual work per unit initial volume. Then $J = 9$, and Eq. (12) implies the Q_j are the components of a stress tensor s_{mn} , say (for large or small strains, Fung (1)). In order to characterize the behavior of laminates using

classical plate theory (22) one may want to associate the set q_j with the middle surface curvatures and strains. In this case, the Q_j would correspond to moments and in-plane forces per unit length, and $\delta(Wk)$ would be virtual work per unit area.

As in the uniaxial example, we assume that when the damage is constant the body (material element, test specimen, or complete structure) is elastic in the usual sense; namely, a work potential W^C exists with the property that

$$Q_j = \partial W^C / \partial q_j \quad (13)$$

(Rather than using the terms "loading" and "unloading" we shall instead now refer to "damaging processes" and "constant damage processes", since we do not want to imply that the damage is always constant when the magnitude of one or more loads or displacements decreases with time.) The effect of damage on Q_j is assumed to be fully represented by a set of "damage parameters"

F_{cn} ($n=1,2,\dots,N$) in the next subsection.

A Special Case: Following Schapery's (20) arguments, it will be shown that for a suitably chosen W^C a work potential W^D exists during damaging processes such that

$$Q_j = \partial W^D / \partial q_j \quad (14)$$

where W^D is a function of only the current values of q_j . One special W^C discussed in (20) is,

$$W^C = W_0(q_j) + \sum_{n=1}^N W_n(F_n, F_{cn}) \quad (15)$$

where W_0 is a work potential without damage effects. It is assumed that all of the functions $F_n = F_n(q_j)$ are such that the N conditions $F_{cn} = F_n$ are satisfied simultaneously during all damaging processes. (The uniaxial case,

Eqs. (3) and (4), is recovered when we set $N=1$ and take $W_0=0$, $F_1 = q_1 = e$, $F_{c1} = e_m$.) To prove that W^D exists, it is necessary and sufficient to show that the generalized forces during damaging processes satisfy

$$\partial Q_j / \partial q_i = \partial Q_i / \partial q_j \quad (i, j = 1, 2, \dots, J) \quad (16)$$

assuming the derivatives in Eq. (16) are continuous (e.g., Greenberg (23)). The forces during a damaging process are taken equal to those in Eq. (13) when $F_{cn} = F_n$ (which is analogous to saying a stress on the loading curve in Fig. 1 is at the upper end of an unloading curve). Consequently, we may evaluate the derivatives in Eq. (16) by first substituting Eq. (15) into (13),

$$Q_j = \frac{\partial W_0}{\partial q_j} + \sum_{n=1}^N \frac{\partial W_n}{\partial F_n} \frac{\partial F_n}{\partial q_j} \quad (17)$$

and then setting $F_{cn} = F_n$ and differentiating Eq. (17) (cf. Eq. (11)),

$$\begin{aligned} \frac{\partial Q_j}{\partial q_i} &= \frac{\partial^2 W_0}{\partial q_j \partial q_i} \\ &+ \sum_{n=1}^N \left[\frac{\partial W_n}{\partial F_n} \frac{\partial^2 F_n}{\partial q_j \partial q_i} + \left(\frac{\partial^2 W_n}{\partial F_n^2} + \frac{\partial^2 W_n}{\partial F_n \partial F_{cn}} \right) \frac{\partial F_n}{\partial q_j} \frac{\partial F_n}{\partial q_i} \right] \quad (18) \end{aligned}$$

Clearly, the right-hand side of Eq. (18) is the same when i and j are interchanged, and therefore Eq. (16) is satisfied.

Generalizations: Extensions of W^C for which W^D exists are discussed in (20), and W^D itself is given. For example, at any given time some of the terms W_n in Eq. (15) may be for constant damage processes while others are for damaging processes. Also, the potentials may depend explicitly on time, and

is not suitable for effects of aging or changing physical environments. (The latter formulation, which allows for large deformations, uses displacement derivatives and strains instead of generalized displacements and forces. However, the earlier formulation, including its extension to viscoelastic behavior (cf. Section 7), carries over fully in terms of the generalized variables used here.) Thus, as in Eq. (8), we may introduce a continuous work potential W for which

$$Q_j = \partial W / \partial q_j \quad (19)$$

even if the damage parameters in some components W_n are constant while others vary in time.

Regardless of the process,

$$\partial Q_j / \partial q_i - \partial Q_i / \partial q_j = 0 \quad (i, j = 1, 2, \dots, J) \quad (20)$$

except at the points of change from one process to another, considering all W_n . The derivatives in Eq. (20) are, in general, discontinuous at these transition points (cf. Fig. 1 at $e = e_m$) and thus Eq. (20) does not apply there. Evidence of transition points may appear in experimental data as significant but somewhat random non-zero values of this difference of derivatives (for $i \neq j$) over short time intervals; this experimental behavior would indicate that a process has changed from one type to another, damaging to constant damage or vice versa.

It is not the goal here to develop specific physical models which give rise to the form for W^c in Eq. (15). We only mention that one based on a simple microcracking model is given by Schapery (20). Also, for characterizing laminates using classical plate theory, each F_{cn} might be proportional to a ply or ply-pair failure surface (such as represented by the Tsai-Wu theory, e.g. (2), expressed in terms of the local ply strains) or

other local invariant. Since the local strains are (linear) functions of the mid-plane strains and curvatures, one obtains $F_n = F_n(q_i)$ if the latter strains and curvatures are included in the set q_i ; the summation in Eq. (15) would extend over all plies.

It is not necessary for the constant-damage potential to have the form in Eq. (15) for the work potential in Eq. (19) to exist. For example, a different form for w^c was given in (20) which contains the Henky deformation theory of plasticity (with elastic unloading). Another example is given in the next subsection.

Micro- and Macrocracking: The work potential W in Eq. (19) may be a constitutive potential in the sense that this equation could be a stress-strain equation for a composite or monolithic material. Alternatively, W may be the total work input to a structure under a general set of boundary displacements q_i whose constitutive response is defined by a work potential density. In either case, the constitutive potential may account for some effects of microcracking, microvoiding, slipping, etc., through the damage parameters F_{CR} . However, the form of the underlying potential w^c for constant damage which has been discussed so far is not completely general. Also, effects of macrocracking (such as large-scale delamination) have not yet been explicitly introduced. Thus, it is of interest to know if a work potential exists when there is macrocracking and a relatively general distribution of growing microcracks. This question will now be examined by embedding additional cracks in the body characterized by W ; the index k will be used to indentify each of these cracks, assumed to be K in number. The cracks may have a wide range of sizes, but it is assumed that the scale of the crack tip failure process zone (which determines the work required for increments of growth) is such that the local material surrounding the failure zone can be

approximated as a continuum, and that the effect of the failure zone on the continuum can be represented by tractions acting along the local crack plane. Then, the virtual work equation with crack growth (see Eq. (13) in (20)), which applies with or without changing damage in the continuum and regardless of whether or not growth is self-similar, gives the available crack tip work per unit of new surface area as $-\delta W/\delta A_k$; δW is the change in the work potential for the total body due to the increase in area δA_k of the k^{th} crack with all q_i fixed. Denoting the available work as G_k , we may thus write

$$G_k = -\partial W/\partial A_k \quad (21)$$

where $k = 1, 2, \dots, K$; also, W is considered to be a function of generalized displacements q_i and oriented crack areas A_k . The quantity G_k is commonly called the energy release rate. The work potential may also depend on damage parameters F_{cn} in that it is the W in Eq. (19) except for the fact that the body now has K additional cracks; the virtual work (Eq. (13) in (20)) from which Eqs. (19) and (21) follow, is shown in (20, p. 222) to be valid with crack growth in bodies with other distributed damage.

In order to predict this growth we also need to specify the work required G_{ck} , say, for a unit of new area of the k^{th} crack area; this quantity is the so-called critical energy release rate. It is not necessary to assume G_{ck} is constant or is the same for all cracks. However, we do assume it can be derived from a fracture work potential $W_f(A_k)$, where

$$G_{ck} = \partial W_f/\partial A_k \quad (22)$$

If for example the critical energy release rate for all cracks is constant, but not necessarily the same,

$$W_f = \sum_{k=1}^K G_{ck} A_k \quad (23)$$

Stable (quasi-static) growth of any one of the K cracks is specified by the condition that required work equals available work, $G_{ck} = G_k$; thus,

$$\partial \bar{W}_f / \partial A_k = -\partial W / \partial A_k \quad (24)$$

If

$$\partial \bar{W}_f / \partial A_k < -\partial W / \partial A_k \quad (25)$$

unstable growth occurs, whereas if

$$\partial \bar{W}_f / \partial A_k > -\partial W / \partial A_k \quad (26)$$

there is no growth.

Returning now to the question of whether or not a work potential exists with crack growth, we shall see that it does for the model defined above if the growth is stable. The potential is denoted as W_T , and it will be shown that it is simply the work of fracture plus the work of deformation of the elastic or inelastic continuum W ; namely,

$$Q_j = \partial W_T / \partial q_j \quad (27)$$

where

$$\bar{W}_T = \bar{W}_f + W \quad (28)$$

The proof is made by first evaluating the derivatives of W_T while allowing for the stable growth of an arbitrary number of the cracks; hence

$$\frac{\partial W_T}{\partial q_j} = \sum_k \left(\frac{\partial \bar{W}_f}{\partial A_k} + \frac{\partial W}{\partial A_k} \right) \frac{\partial A_k}{\partial q_j} + \frac{\partial W}{\partial q_j} \quad (29)$$

For those cracks which do not grow, $\partial A_k / \partial q_j = 0$. In view of Eq. (19) as well as Eq. (24) for the growing cracks, Eq. (29) reduces to Eq. (27), which was to be shown.

Equation (24) is a set of K' ($0 < K' < K$) equations whose solution gives the areas $A_k(q_j)$ of K' growing cracks in terms of the generalized displacements.

If we assume a unique solution exists (at least for small changes in q_i) then the areas (or their changes) could be substituted into W_f and W in Eq. (28). In this form W_T would be a function of q_j and only those A_k which are constant.

Pursuing this representation further, let us suppose for simplicity that all areas A_k are simultaneously either constant or vary; denote the constant values by A_{ck} . Then for a constant damage process (apart from possible effects of F_{cn} and F_n),

$$W_T^C = W_T(q_j, A_{ck}) \quad (30)$$

and for a damaging process, $A_{ck} \rightarrow A_k(q_j)$,

$$W_T^D = W_T(q_j, A_k(q_j)) \quad (31)$$

Equation (30) does not necessarily have the special form of Eq. (15), but yet a work potential exists for constant and changing damage; the limitation is instead in the form of the relationship governing $A_k(q_i)$, viz. Eq. (24).

Unstable Crack Growth: Unstable crack growth occurs when $G_k > G_{ck}$. The excess work predicted from quasi-static analysis is then modified by dynamic effects, and the quantity W_T in Eq. (28) is not equal to the work input to the body. This does not necessarily mean a work potential does not exist. In fact, the assumption of quasi-static crack growth was not used to arrive at Eq. (19). The functions $F_n(q_j)$ may reflect, at least in part, an average effect of unstable rapid steps of microcrack growth.

Significance of the Areas A_k : Through principles of fracture mechanics we obtained a work potential W_T , and furthermore related it to physically identifiable parameters A_k and material-related functions W_f and W . Conceptually, all cracks are considered to pre-exist with given initial sizes and orientations; but many or all may be so small initially that they have no

real effect on the work potential. In principle, as many A_k are to be used as are needed to fully define the instantaneous location and orientation of all crack surfaces and their growth. For example, a crack edge that advances nonuniformly along its length may require the use of many small areas or parameters A_k to define the changing geometry. With complex arrays of cracks this formulation is not practical unless idealizations, such as periodicity and regular shapes, or statistical representations are introduced. Non-unique solutions $A_k(q_j)$ would further complicate the problem, giving rise to effects of the history $q_i(t)$. In such a case, one may have to solve for changes in A_k using small changes in q_i . Of course, our purpose was simply to argue that a work potential exists; nevertheless, it should be recognized that even with a work potential, there could be effects of the displacement history. Additional complications could arise with friction between adjacent crack faces, in that a work potential does not always exist if there is appreciable energy dissipation through sliding processes; however, it should be recalled that significant plastic deformation (slip) processes may occur in metals and yet a potential exists for some histories, as modeled by the deformation theory of plasticity.

One could think of the parameters A_k as "internal variables", such as used in irreversible thermodynamic formulations; they need not be areas as long as they fit the above mathematical model. Although it is not necessary here, we may write the equations which govern their growth, Eq. (24) or equivalently $G_{ck} = G_k$, in a rate form similar to that used in thermodynamic models. First differentiate $G_{ck} = G_k$ with respect to time,

$$\sum_m \frac{\partial G_{ck}}{\partial A_m} \frac{dA_m}{dt} = \sum_m \frac{\partial G_k}{\partial A_m} \frac{dA_m}{dt} + \sum_j \frac{\partial G_k}{\partial q_j} \frac{dq_j}{dt} \quad (32)$$

where, for simplicity, explicit time-dependence (e.g. aging) in G_{ck} and G_k is omitted.

Solve for dA_m/dt ,

$$\frac{dA_m}{dt} = \sum_{k,j} H_{mk} \frac{\partial G_k}{\partial q_j} \frac{dq_j}{dt} \quad (33)$$

where H_{mk} is the inverse of the matrix G_{km} ,

$$G_{km} \equiv \partial G_{ck} / \partial A_m - \partial G_k / \partial A_m \quad (34)$$

Complementary Work Potential: In many problems it is desirable to use the Q_j instead of q_j as the independent variables. All of the preceding theory could have been formulated in this way, in which a complementary work potential W_C , say, would be used, where

$$q_j = \partial W_C / \partial Q_j \quad (35)$$

For the one-dimensional case in Fig. 1, W_C is the area to the left of the curves,

$$W_C = \int_0^s e \, ds' \quad (36)$$

where $e = f(s', s_m)$ or $e = f(s', s')$, depending on the curve to be used, and s_m is the maximum stress. The relationship between W_T and W_C is

$$W_T + W_C = \sum_{j=1}^J Q_j q_j \quad (37)$$

Observe that we may start with Eq. (27) and then define W_C by Eq. (37); differentiation of the latter equation yields Eq. (35). Alternatively, we could reverse the process. Thus, if W_T exists so does W_C , and vice-versa. It should be noted that these potentials are multivalued, and therefore one has to interpret their interrelationships on a process-by-process basis. For instance, in identifying a particular (s,e) pair for the example in Fig. 1, it is obviously necessary to specify whether the loading or unloading curve is to be used.

4. Angle-Ply Composite Bars under Axial and Torsional Loading

The theory in Section 3 provides support for using work potentials

to characterize the behavior of materials and structures with damage. In this and the next two Sections we describe studies of polymeric composite materials which give preliminary experimental confirmation of this characterization for damaging processes.

Work using laminates of graphite fiber-reinforced epoxy under axial and torsional loading is described in this Section. The tests specimens are flat bars, as illustrated in Fig. 2, which consist of several plies or layers, each being a relatively brittle, elastic composite with continuous, unidirectional fibers having an angle θ with respect to the bar's axis; $\theta = \pm 30^\circ$ are used in the specimens discussed here. The unidirectional material was supplied in pre-preg form by Hercules, Inc., and is designated as AS4/3502. It should be emphasized that even though there are strain gradients and consequent nonuniform damage (primarily in the form of distributed microcracks and, at high loads, edge delaminations) the theory in Section 3 may be used. (Basic stress-strain behavior using thin-walled tubes will be studied in the near future after acquiring additional laboratory equipment.)

The generalized variables of Section 3 will be identified with the specific mechanical variables for the bar as follows: axial elongation, $u = q_1$; rotation angle between ends, $\Omega = q_2$; axial load, $F = Q_1$; and torque, $T = Q_2$. The total work potential W_T , Eq. (28), is the work input to the entire bar through the relatively rigid grips.

The necessary and sufficient conditions for existence of a potential, Eq. (16), for the present problem reduce to the single equation,

$$\partial F / \partial \Omega = \partial T / \partial u \quad (38)$$

Before using Eq. (38) with experimental data, it is helpful to replace the variables by measures of stress and strain. This normalization process

eliminates first-order effects of specimen-to-specimen dimension differences. Specifically, we shall use "nominal" stresses and strains defined as

$$\begin{aligned} s &\equiv F/bc & \tau &\equiv 3T/bc^2 \\ e &\equiv u/L & \gamma &\equiv c\Omega/L \end{aligned} \quad (39)$$

where b = width, c = thickness, and L = length (between grips). For the special case of long, thin homogeneous specimens ($L \gg b \gg c$) s and e are the uniform axial stress and strain respectively, and τ and γ are the in-plane shear stress and strain respectively at the surface. This is shown by Timoshenko (24) for linear isotropic materials; for orthotropic materials whose planes of symmetry are parallel to the specimen surfaces, it can be shown that the same formulas apply except the width is modified by a ratio of moduli. The shear strain magnitude is zero at the mid-plane and increases linearly to the specimen faces ($L \times b$) in Fig. 2. Whether or not the stated conditions apply the variables in Eq. (39) are useful for normalizing data. Equation (38) becomes

$$\partial s / \partial \gamma = \partial (\tau/3) / \partial e \quad (40)$$

This equation has been used to analyze the data in Figs. 3 and 4 by first writing

$$\tau/3 = \tau_0/3 + g \quad (41)$$

where $\tau_0 = \tau_0(\gamma)$ is the shear stress for $e=0$; also $g=g(e,\gamma)$ in which $g(0,\gamma) = 0$. Next, integration of Eq. (40) with respect to γ yields

$$s = \frac{\partial}{\partial e} \int_0^\gamma g(e,\gamma') d\gamma' + s_0 \quad (42)$$

where $s_0 = s_0(e)$ is the axial stress when $\gamma=0$. Thus, the quantity

$$\Delta s \equiv \frac{\partial}{\partial e} \int_0^{\gamma} g(e, \gamma') d\gamma' \quad (43)$$

is the change in axial stress due to the twist induced shear strain. This integrated form is to be preferred over the original Eq. (40) because of the inaccuracy resulting from differentiation of experimental data, considering especially the small amount of data available.

The procedure used to check for the existence of a work potential was to cross-plot the data in Fig. 3 so as to obtain g (which is proportional to the change in shear stress due to axial strain) as a function of γ , for fixed values of e , and then predict the modification to axial stress, Eq. (43). Considering the limited amount of data available, it is desirable to curve fit analytical expressions to the data to aid the needed interpolations and extrapolations. It was found for a wide range of strains that

$$\int_0^{\gamma} g(e, \gamma') d\gamma' = A\gamma^{2.55} e^{(B+C\gamma)} \quad (44)$$

where A, B , and C are constants. Using this expression in Eq. (43) yields the change in axial stress due to twist. Only for $e/\gamma = 0.92$ is there a significant effect of twist prior to fracture; the prediction is drawn in Fig. 4. The agreement between theory and experiment is relatively good.

In the series of tests shown in Figs. 3 and 4 there is only one specimen for each deformation history, and thus the small differences between most curves in Fig. 4 could be as large as specimen-to-specimen differences. Nevertheless, it is encouraging that all of the predictions from Eq. (43) turned out to be of the same order as the observed differences in axial stress. Axial stress for $\gamma=0$ is not shown, but it was essentially the same as for $e/\gamma = 1.78$ in Fig. 4 until premature failure occurred; the latter results were used in the theoretical predictions. Although not needed to check for the existence of a potential, it is of interest to observe that when there is little or no coupling effect of twist and axial deformation, the stress-strain

curves obey power laws over a wide range of strains; this is shown in Fig. 5 where

$$s \sim e^m \quad \text{and} \quad \tau \sim \gamma^n \quad (45)$$

We have conducted additional exploratory tests using proportional straining of laminates with various widths, thicknesses, and fiber angles, all of the angle-ply design ($\pm\theta$) with balanced, symmetric layups. The behavior is similar to that already discussed, with comparable verification of Eq. (43). Close to the end point of the curves, where large scale delamination or failure at the grips occurs, theoretical and experimental curves tend to separate, as seen in Fig. 4. This difference may possibly be due to inaccuracy in the extrapolations needed for Eq. (43) (considering the small number of specimens used), a change from damaging to constant damage processes and vice versa (cf. discussion of Eq. (20)), or an inability to use a potential in a highly damaged state. Future studies using proportional and nonproportional straining should help to explain this behavior.

For some layups with sufficient twist, mode III edge delamination occurs prior to significant material fracture near the grips. As a result, properly designed bar specimens with and without initial delaminations may be useful for studies of this type of delamination. When a work potential exists, one often can use the J integral theory or energy release rates to account for the effect of distributed damage on the delamination growth.

5. A Highly-Filled Elastomer under Axial Loading and Pressure

Several years ago Farris (25) described large deformation studies of crosslinked rubber containing 65 volume percent of relatively hard particles. Specimens in the shape of slender rectangular bars were subjected to confining pressure and uniaxial loading. He used reversible thermodynamics as a basis

for predicting the effect of pressure on the axial stress-strain behavior. These predictions were in quite good agreement with the measurements, in spite of strong effects from the irreversible processes of microcracking and void growth. Here we re-examine the behavior and use the present work potential theory as a basis for making similar predictions.

The specimen and relatively rigid grips are shown schematically in Fig. 6. This assembly was placed in a chamber, where it was first pressurized to a constant value p and then stretched axially at a constant crosshead rate; the axial force acting on the grips is F . Representative stress-strain and dilatation-strain data are in Fig. 7.

In order to select the generalized variables in Eq. (12), we use for $\delta(Wk)$ a virtual work per unit initial specimen volume,

$$\delta(Wk) = \frac{1}{V_0} \int_A \mathbf{T} \cdot \delta \mathbf{u} dA \quad (46)$$

where \mathbf{T} and $\delta \mathbf{u}$ are the surface traction and virtual surface displacement vectors, respectively, and V_0 is the initial specimen volume; the integration is over the instantaneous area A of the specimen and rigid grips. On all surfaces except on the grip ends where F is applied,

$$\mathbf{T} = -p \mathbf{n} \quad (47)$$

in which \mathbf{n} is the outer unit normal to the surface. It is helpful to write the normal traction on the grip ends in the form

$$T_n = T_1 - p \quad (48)$$

where T_1 is defined by this equation. Integrating $T_n dA$ over the grip ends with area A_g , regardless of whether or not T_n is uniformly distributed, gives the axial force as

$$F = F_1 - p A_g \quad (49)$$

where

$$F_1 \equiv \int_{A_g} T_1 dA \quad (50)$$

is the axial force above that due to the pressure. Equations (47), (48), and (50), along with the assumption of purely axial movement of the grips, reduce Eq. (46) to

$$\delta(Wk) = \frac{F_1}{V_0} \delta u_1 - p \frac{\delta V}{V_0} \quad (51)$$

where δu_1 and δV are the virtual axial elongation and volume change of the specimen, respectively. Let us now choose for generalized displacements the nominal axial strain, e , and dilatation, v , defined in the usual way,

$$q_1 = e \equiv u_1/L_0, \quad q_2 = v \equiv V/V_0 \quad (52)$$

where u_1 and V are the increases in specimen length and volume from the initial unstrained state (in which the length is L_0 and volume is V_0). Comparing Eqs. (12) and (51) we see that the generalized forces are

$$Q_1 = s, \quad Q_2 = -p \quad (53)$$

where $s \equiv F_1/A_0$, the "nominal stress".

As in Section 4, we shall use Eq. (16) (with $i=2$, $j=1$) in integrated form to determine if a potential exists. Namely, substitute the variables from Eqs. (52) and (53) and integrate with respect to v ,

$$s(e,v) = - \frac{\partial}{\partial e} \left(\int_{v_0}^v p dv \right) + s(e,v_0) \quad (54)$$

where v_0 is a constant reference value of dilatation. This result is equivalent to that used by Farris except for an additional term arising from surface or fracture energy, which he attributed to the formation of vacuoles. However, he subsequently neglected this term and then used the theory and crossplots constructed from data in Fig. 7 to make the predictions in Fig. 8.

For $s(e, v_0)$ the curve for $p = 500$ psi was used; although the dilatation is not constant in this case, it is very nearly so (cf. Fig. 7).

It should be noted that Eq. (54) is correct as it stands, in that surface or fracture energy changes are taken into account implicitly when one uses data for damaging processes. The underlying potential is W_T , Eq. (28), which consists of the work of fracture W_f plus the deformation work W . Furthermore, no restriction has been imposed on the magnitude of the strain or its uniformity; the strains are in fact quite large, and are nonuniform at least close to the grips.

The agreement between results from experiment and potential theory is seen in Fig. 8 to be quite good. The discrepancy is relatively small compared to the differences between the various stress-strain curves and that at 500 psi; the error that does exist may be largely due to the moderate amount of viscoelasticity exhibited by this material. Note that the extent of damage is large at the low pressures, in the sense that without microcracking and the subsequent development of microcavities the dilatation would be negligible compared to the values in Fig. 7; also, the uniaxial stress-strain curves would be pressure-insensitive since, with increasing pressures, the curves approach that for essentially zero dilatation.

The results in Figs. 7 and 8 are from tests conducted at constant pressure. Farris also gave the results in Fig. 9, which include a test in which the pressure was initially at 500 psi, and then, while the sample was being strained, the pressure was suddenly lowered to 40 psi; following additional straining, it was increased to 500 psi. It is seen that after a short period of time following each pressure change, the stress-strain curve tends to approach the one for which the pressure was constant during the

entire straining period. In other words, there is not a strong effect of pressure history in this case.

6. Delamination in Double Cantilevered Beams

The symmetric split beam test depicted in Fig. 10 is now commonly used to determine the critical energy release G_c for the opening mode of delamination of fiber-reinforced plastics. When there is a significant volume fraction of fibers which are not parallel to the beam axis the two legs may be highly inelastic, thus invalidating the standard elastic methods used to obtain G_c from experimental data on load, deflection, and crack length. As an illustration of the use of the potential theory in Section 3 for fracture analysis, we shall derive an equation for determining G_c in inelastic beams.

It turns out that the complementary work potential W_c , Eq. (35), is used more conveniently for this problem than the work potential. In the formulation we shall employ, the potential W_T in Eq. (37) will include the fracture work of all microcracks but not that of the delamination. For this case the work that becomes available at the delamination crack tip for a unit of new area of surface A (projected onto the delamination plane), is given by

$$G = \partial W_c / \partial A \quad (55)$$

where the derivative is taken with generalized forces held constant. This formula can be derived by first observing that the total variation of Eq. (37) may be written in the form

$$\left(\frac{\partial W_T}{\partial A} + \frac{\partial W_c}{\partial A} \right) \delta A = \sum_{j=1}^J \left[\left(Q_j - \frac{\partial W_T}{\partial q_j} \right) \delta q_j + \left(q_j - \frac{\partial W_c}{\partial Q_j} \right) \delta Q_j \right] \quad (56)$$

The right side vanishes by virtue of Eqs. (27) and (35), and therefore

$\partial W_c / \partial A = -\partial W_T / \partial A$. Equation (21) then yields Eq. (55) since we may use Eq. (21) for the delamination crack in which the work potential is W_T instead of

W, allowing for the work of microcrack extension introduced in Eq. (28).

For the DCB specimen in Fig. 10, let $F = Q_1$ and $2u = q_1$. Use a and b to define the instantaneous crack length and specimen width referred to the unstrained (flat beam) geometry and then take $A = ab$. The complementary work for the total test specimen is

$$W_C = W_C(F, a) = 2 \int_0^a w_c dx_1 + W_C' \quad (57)$$

where x_1 is a coordinate axis along the specimen centerline (which defines the location of material points in the unstrained geometry) and $x=0$ is at the initial line of load application. The quantity w_c is defined as the complementary work density (based on unit length) for each leg from classical beam theory: namely, the theory based on the assumption that material planes which are initially normal to the beam axis remain plane and normal when the beam is deformed. The correction to beam theory is denoted by W_C' . The energy release rate becomes

$$G = \frac{1}{b} \frac{\partial W_C}{\partial a} = \frac{2}{b} w_c(a) + \frac{2}{b} \int_0^a \frac{\partial w_c}{\partial a} dx_1 \quad (58)$$

after neglecting $\partial W_C'/\partial a$. For long beams W_C' is primarily from distortion of the beam immediately to the right of the delamination crack tip, and $\partial W_C'/\partial a$ can be shown to vanish if the beam is long enough that the crack tip is essentially isolated from the ends.

Equation (58) is not restricted to small strains and rotations. As such, the horizontal distance a' in Fig. 10 may be significantly less than the actual length of the crack surface a . However, we shall simplify the analysis

by assuming small strains and rotations and further assume both legs are symmetric and balanced laminates in the undamaged and damaged states. With these conditions there is no mid-plane stretching or twisting, and beam theory gives the simple result

$$w_c = \int_0^M k dM' \quad (59)$$

where $k = k(M')$ is the curvature as a function of the moment. A moment-curvature diagram for inelastic material would be similar to the stress-strain diagram in Fig. 1; the complementary work, Eq. (59), is thus to be evaluated taking into account the multivalued relationship, as discussed in Section 2. The local beam moment is

$$M = Fx_1 \quad (60)$$

and therefore the integral in Eq. (58) vanishes as w_c is independent of a . Thus, we obtain

$$G = \frac{2}{b} w_c(a) = \frac{2}{b} \int_0^{M_a} k(M) dM \quad (61)$$

where $M_a = Fa$ is the crack tip moment.

This result has been used by Jordan (26) to analyze delamination of two different graphite/epoxy material systems with plies having various fiber orientations; one system had a rubber-toughened resin and the other a brittle resin system. Figure 11 gives a typical load-displacement diagram for the latter one. The short inclined lines represent periods of no crack growth following sudden jumping at loads along the dashed line. Measurement of crack length and corresponding loads indicated that the crack tip moment at the beginning of each jump in crack length was approximately constant for all tests in the series. Four-point bend tests were used to develop the moment-

curvature diagram of beams with the layup of one-half of the DCB specimen (i.e. for one leg). Knowing the moment for crack growth from the DCB tests and the moment-curvature diagram from the four-point bend tests made it possible to derive the critical energy release rate from Eq. (61); the average moment at which crack jumping occurred for each DCB specimen was used for M_a . This calculation, which is illustrated in Fig. 12, gave values for G_c which were practically the same for all layups of each of the two graphite/epoxy systems. Indeed, the G_c for unidirectional ($\theta=0^\circ$) laminates was close to that of the layup with multiple fiber orientations. In contrast, standard data analysis based on beam deflection and load gave G_c values which differed considerably for the several layups; some multiple-fiber angle layups had apparent G_c values over twice that for $\theta=0$.

These findings not only help to support the underlying potential theory, but also reveal surprisingly simple behavior, considering especially how much microcracking develops in the specimens whose bending is not fiber-dominated. The layup insensitivity of G_c seems to indicate that the local normal interface stress, rather than local layup-induced shear stress, is the primary factor in delamination. Of course, the findings are from a limited set of tests on only two composite systems, and therefore one should be cautious about extrapolating the findings to other laminates.

Finally, it is of interest to consider the relationship of the above results to Rice's J integral (19), as extended to crack growth in inelastic media with large deformations by Schapery (20). The quantity J is defined by a contour integral, which becomes for the beam problem in Fig. 13,

$$J = \int_C [w_0 dx_2 - (T_1 \frac{\partial u_1}{\partial x_1} + T_2 \frac{\partial u_2}{\partial x_1}) dL] \quad (62)$$

where w_0 is the work potential density, T_1 and T_2 are tractions along C , and u_1 and u_2 are displacements; the indices indicate components in the x_1 and x_2 directions. This equation is valid for large strains and rotations as long as we interpret x_1 and x_2 to be coordinates of the undeformed geometry. The integration is counterclockwise along the curve C in Fig. 13, which includes top and bottom beam surfaces and vertical segments. The right vertical segment is taken far enough from the crack tip that the material is unstressed, and thus gives no contribution. For the top and bottom segments, $dx_2 = T_1 = T_2 = 0$, and thus the only contribution comes from the left segment. Assuming small strains and that the left segment is close enough to the crack tip that we can use small rotation beam theory, yields,

$$J = \frac{2}{b} \int_0^M k(M') dM' - 2 \frac{F}{b} \frac{du_2}{dx_1} \quad (63)$$

where M and du_2/dx_1 are the moment and slope, respectively, at the left vertical segment. Integrate $k = d^2u_2/dx_1^2$ to obtain the slope, and Eq. (63) reduces to

$$J = \frac{2}{b} \int_0^{M_a} k(M) dM \quad (64)$$

where M_a is the crack tip moment; this is the same result derived by Rice (19) for a split beam under end moments M_a . It is seen that the result is independent of the location of the left integration segment and, in fact, is that in Eq. (63) when the segment is located at the crack tip (where $du_2/dx_1 = 0$). It should be mentioned, however, to obtain this path independence (i.e. derive Eq. (64) from (63)) it was necessary to assume if $k(M)$ is multivalued (cf. Fig. 1) that the unloading curve is the same for all left vertical segments used. This latter condition will be met for all material (to the left of the current tip) which had experienced the same maximum moment

when the crack tip passed by. Inasmuch as the experimental results discussed above indicate the maximum moment is constant (and recognizing that the moment decays with distance from the tip) this condition is met all of the way to the location of the initial crack tip. To the left of the initial tip, the maximum moment is less than M_a and one finds J depends on the location of the left segment. This path dependence in beam theory is fully consistent with that predicted from the exact J integral for a continuum with variable damage in the regions of unloading (20). Some unloading may occur in the continuum very close to the crack tip, possibly causing path dependence and thus affecting Eq. (64). Weatherby (27) used a finite element analysis to study this dependence for a strongly nonlinear isotropic beam and found that the effect on J is negligible; his analysis predicted a J value very close to that in Eq. (64).

For a crack propagating at a constant moment in a long laminate which is initially homogeneous in the x_1 direction, the state of stress and strain in the neighborhood of the tip is constant in time. This is a type of "self-similar" growth and therefore (19,20)

$$G = J \quad (65)$$

Equations (61) and (64) agree with this general result. Equally important, Eq. (64) was derived without assuming small rotations (except for the neighborhood of the tip). Therefore, in view of Eq. (65), we may conclude that the formula for work available at the crack tip, Eq. (61), is valid even when the DCB legs undergo large rotations and possibly high axial tensile strains from the axial component of F . When this geometric nonlinearity exists one should use a' (cf. Fig. 10) instead of a to determine the crack tip moment.

7. Viscoelastic Behavior

For some types of linear and nonlinear viscoelastic materials the theory

in Section 3 may be used by simply replacing the generalized displacements with "pseudo generalized displacements," q_j^R , where

$$q_j^R \equiv E_R^{-1} \int_0^t E(t-\tau, t) \frac{\partial q_j}{\partial \tau} d\tau \quad (66)$$

Here q_j is the physical generalized displacement in terms of the dummy time variable of integration τ and other relevant quantities such as coordinates x_i . The quantity $E = E(t-\tau, t)$ is a relaxation modulus, which imparts hereditary characteristics to the deformation behavior. The second t argument in E allows for aging and other kinds of time-dependence, such as may be due to transient temperature. The coefficient E_R is a "reference modulus", which is an arbitrarily selected constant that is introduced so that q_j^R and q_j have the same units. The basis for using Eq. (66) to extend deformation and crack growth theory to viscoelastic behavior has been given by Schapery (15,20). Here we mention only that it is an exact approach for linear isotropic viscoelastic materials with a Poisson's ratio which is constant in the undamaged state and for nonlinear viscous materials. The latter case is easily deduced by noting that if the relaxation modulus is proportional to a Dirac delta function, i.e. $E = E_R t_R \delta(t-\tau)$, where t_R is a time constant, then Eq. (66) reduces to

$$q_j^R = t_R dq_j/dt \quad (67)$$

Namely, the pseudo displacement is proportional to velocity with this modulus choice. Replacement of q_j by this q_j^R in Eqs. (19), (27), and (35) converts them to equations for viscous media.

Elastic-viscoelastic correspondence principles were developed (15,20) which then lead to the development of the theories for effective properties of

composites (15) and crack and damage growth (20). To date only limited, but encouraging, experimental work on nonlinear viscoelastic materials has been done to verify this approach based on pseudo displacements (Schapery (28,29)). In study (29), a highly-filled elastomer was subjected to complex uniaxial loading histories. The experimentally measured axial displacement u of tensile coupons was converted to nominal strain e and then to pseudo strain e^R using Eq. (66), and the axial stress was plotted against e^R for constant damage states. It was found that this method of plotting data essentially eliminated viscoelastic effects, thus confirming the approach. For damaging processes, the material behaved as a nonlinear elastic material with history-dependent damage when represented in terms of e^R . Guided by simple models for damage and some test data, the nonlinear viscoelastic stress-strain equation was developed and then verified experimentally using loading histories not included in the characterization process.

Besides employing the maximum value e_m^R to account for damage, as e_m is used in Eq. (3), a so-called Lebesgue norm was used in (29),

$$L_q \equiv \left[\int_0^t |e^R|^q dt \right]^{1/q} \quad (68)$$

where $|\cdot|$ denotes absolute value and q is a positive constant; the damage parameter L_q arises from viscoelastic crack growth theory. If q is sufficiently large, L_q (and its generalization to multidimensional problems) may often lead to constitutive equations which are analogous to those discussed in Sections 2 and 3; but there may be explicit dependence of the potentials W , W_f , and W_c on time, and thus they would be like those for aging elastic materials with damage. For example, $e^R \geq 0$ and $q = 6.5$ in (29), and in this case,

$$L_q \approx e^R t^{1/q} \quad \text{when } de^R/dt > 0 \quad (69)$$

and

$$L_q \approx e_m^R t^{1/q} \quad \text{when } de^R/dt = 0 \quad (70)$$

If e^R reaches a maximum at $t=t_m$ and then decreases,

$$L_q \approx e_m^R t_m^{1/q} \quad (71)$$

Behavior like that in Eqs. (69) and (70) reflects the growth of microcracks until the "driving force" e^R falls below its maximum value.

8. Conclusions

An approach using work potentials to characterizing deformation and fracture behavior of inelastic materials has been described. Some experimental results on polymeric composites were presented to illustrate it and give a preliminary verification of the theory. If the use of work potentials to account for the effect of damage and other types of inelasticity is further substantiated in future studies, one may take advantage of the simplifications that come from this approach in the mathematical modeling of both deformation and fracture behavior. When pseudo displacements, Eq. (66), can be used to extend the time-independent characterization to nonlinear viscoelastic behavior, additional experimental requirements and mathematical model complexity are not much more than what is needed for linear viscoelastic behavior.

Acknowledgement

This author is grateful to the U.S. Air Force of Scientific Research, Office of Aerospace Research, for sponsoring this work, and to Mr. Mark Lamborn, graduate research assistant, for doing the axial-torsional testing of laminates and data analysis.

REFERENCES

1. Y.C. Fung, "Foundations of Biomechanics," Prentice-Hall, Inc., Englewood Cliffs, New Jersey (1973).
2. Z. Hashin, J. Appl. Mech., 37, 471 (1970).
3. M. Kachanov, J. Eng. Mech., ASCE, 106, 1 (1980).
4. R. Hill, J. Mech. Phys. Solids, 5, 66 (1956).
5. M.A. Biot, Phys. Rev., 97, 1463 (1955).
6. T.G. Rogers and A.C. Pipkin, LAMP, 14, 334 (1963).
7. R.A. Schapery, J. Compos. Mater., 1, 228 (1967).
8. J.R. Rice, J. Appl. Mech., 37, 728 (1970).
9. J.M. Dupa and J.W. Hutchinson, Mechanics of Materials, 3, 41 (1984).
10. L.E. Malvern, "Introduction to the Mechanics of a Continuous Medium," Prentice-Hall, Inc., Englewood Cliffs, New Jersey (1969).
11. J.R. Rice, J. Mech. Phys. Solids, 19, 433 (1971).
12. B.D. Coleman and M.E. Gurtin, J. Chem. Phys., 47, 597 (1967).
13. R.A. Schapery, "Further Development of a Thermodynamic Constitutive Theory: Stress Formulation." AA & ES Report No. 69-2, Purdue Univ. (1969).
14. R.A. Schapery, In "Thermoinelasticity," (B.A. Boley, ed.) Springer-Verlag, New York, 259 (1970).
15. R.A. Schapery, In "1981 Advances in Aerospace Structures and Materials," (S.S. Wang and W.J. Renton, eds.) The American Society of Mechanical Engineers, New York, 5 (1981).
16. D. Broek, "Elementary Engineering Fracture Mechanics," Third Ed., Martinus Nijhoff Publishers, Boston (1982).
17. G.J. Lake, In "Progress of Rubber Technology", Applied Science Publishers Ltd., London, 89 (1983).

18. E.H. Andrews, J. Mater. Sci., 9, 887(1974).
19. J.R. Rice, J. Appl. Mech., 35, 379(1968).
20. R.A. Schapery, Int. J. Fracture, 25, 195(1984).
21. M.E. Gurtin and E.C. Francis, J. Spacecraft and Rockets, 18, 285(1981).
22. R.M. Jones, "Mechanics of Composite Materials," Scripta Book Co., Washington D.C. (1975).
23. M.D. Greenberg, "Foundations of Applied Mathematics", Prentice-Hall, Inc., Englewood Cliffs, New Jersey, 170(1978).
24. S.P. Timoshenko and J.N. Goodier, "Theory of Elasticity," Third Ed., McGraw-Hill Book Co. (1970).
25. R.J. Farris, Trans. Soc. Rheol., 12 2, 303(1968).
26. W.M. Jordan, "The Effect of Resin Toughness on the Delamination Fracture Behavior of Graphite/Epoxy Composites," Ph.D. Dissertation, Interdisciplinary Eng'g, Texas A&M Univ. (Dec. 1985).
27. J.R. Weatherby, "Finite Element Analysis of Crack Growth in Inelastic Media," Ph.D. Dissertation, Mechanical Eng'g, Texas A&M Univ. (May 1986).
28. R.A. Schapery and M. Riggins, In "Numerical Models in Geomechanics", (R. Dungar, G.N. Pande, and J.A. Studer, eds.) A.A. Balkema, Rotterdam, 172(1982).
29. R.A. Schapery, "Proc. Ninth U.S. Nat. Cong. Appl. Mech.," Book No. H00228, ASME, New York, 237(1982).

NOMENCLATURE

a	crack length
A, A_k	crack areas
b	beam width
e	nominal strain (axial extension/initial length)
e_{ij}	strain tensor
$E(t-\tau, t)$	relaxation modulus
F	force
F_n	damage function
F_{cn}	damage parameter
G, G_k	energy release rates
G_c, G_{ck}	critical energy release rates
J	J integral
k	curvature
L	beam length
L_q	Lebesgue norm
M	moment
p	pressure
q_j	generalized displacement
Q_j	generalized force
s	nominal stress (axial stress/initial cross sectional area)
s_{ij}	stress tensor
t	time
T	torque
u	displacement
v	dilatation

V	increase in volume
V_0	initial volume
w_c	complementary work density
W_c	complementary work potential
w, w_T	work potentials
w_f	fracture work potential
x_i	Cartesian coordinates
γ	nominal shear strain
τ	nominal shear stress
Ω	angle of twist

V	increase in volume
V_0	initial volume
w_c	complementary work density
\bar{w}_c	complementary work potential
\bar{w}, \bar{w}_T	work potentials
\bar{w}_f	fracture work potential
x_i	Cartesian coordinates
γ	nominal shear strain
τ	nominal shear stress
Ω	angle of twist

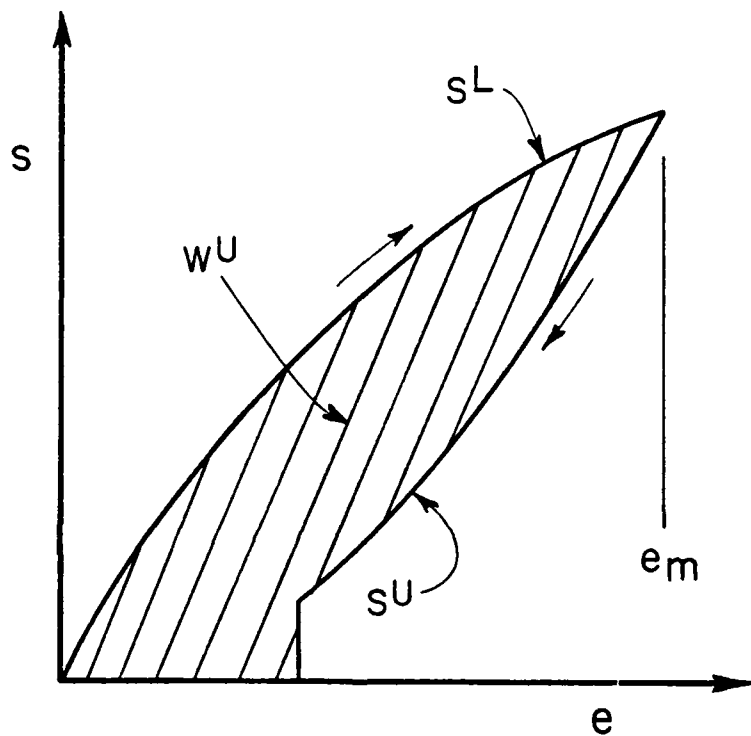


Figure 1. Uniaxial stress-strain curve for material with increasing damage during loading and constant damage during unloading.

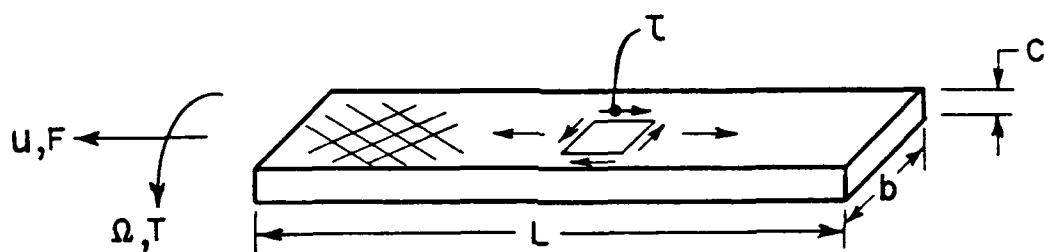


Figure 2. Laminate specimen used in axial-torsional tests.

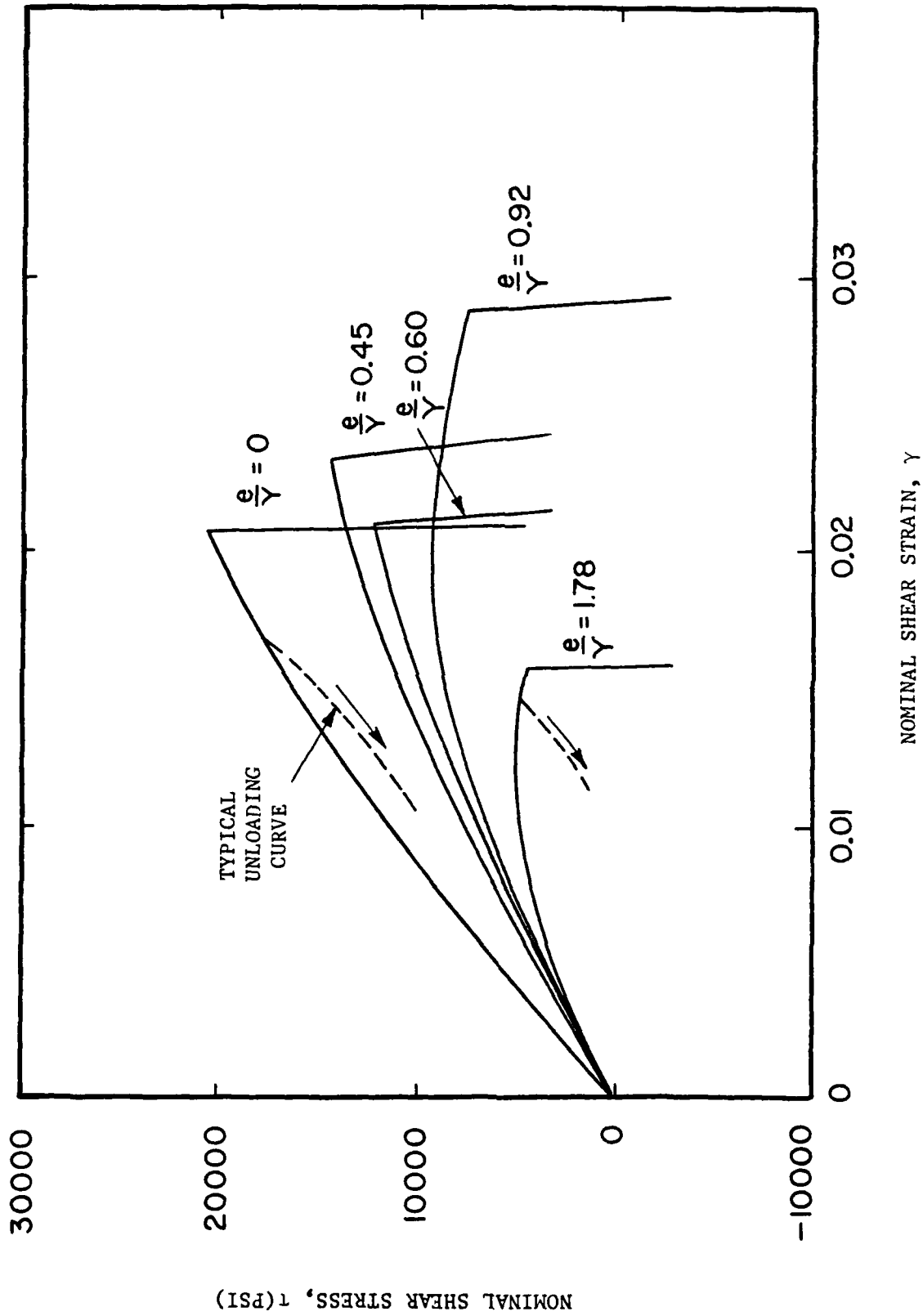


Figure 3. Representative shear stress-strain curves with proportional axial and torsional straining. Hercules AS4/3502 graphite/epoxy; 24 plies $[+30]_{6S}$; 2.5 in. long x 0.25 in. wide x 0.13 in. thick.

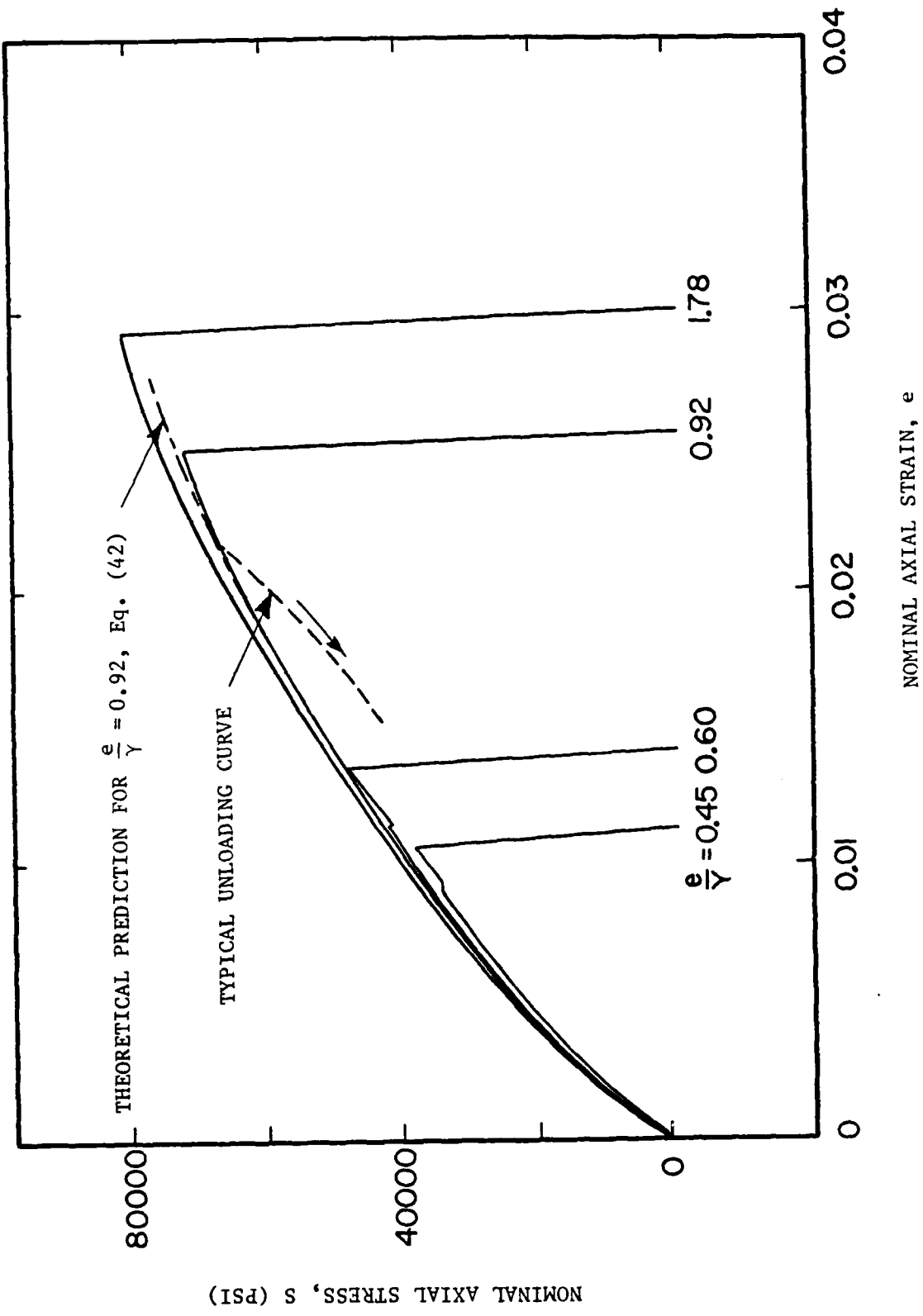


Figure 4. Representative axial stress-strain curves with proportional axial and torsional straining from the same tests used for Figure 3.

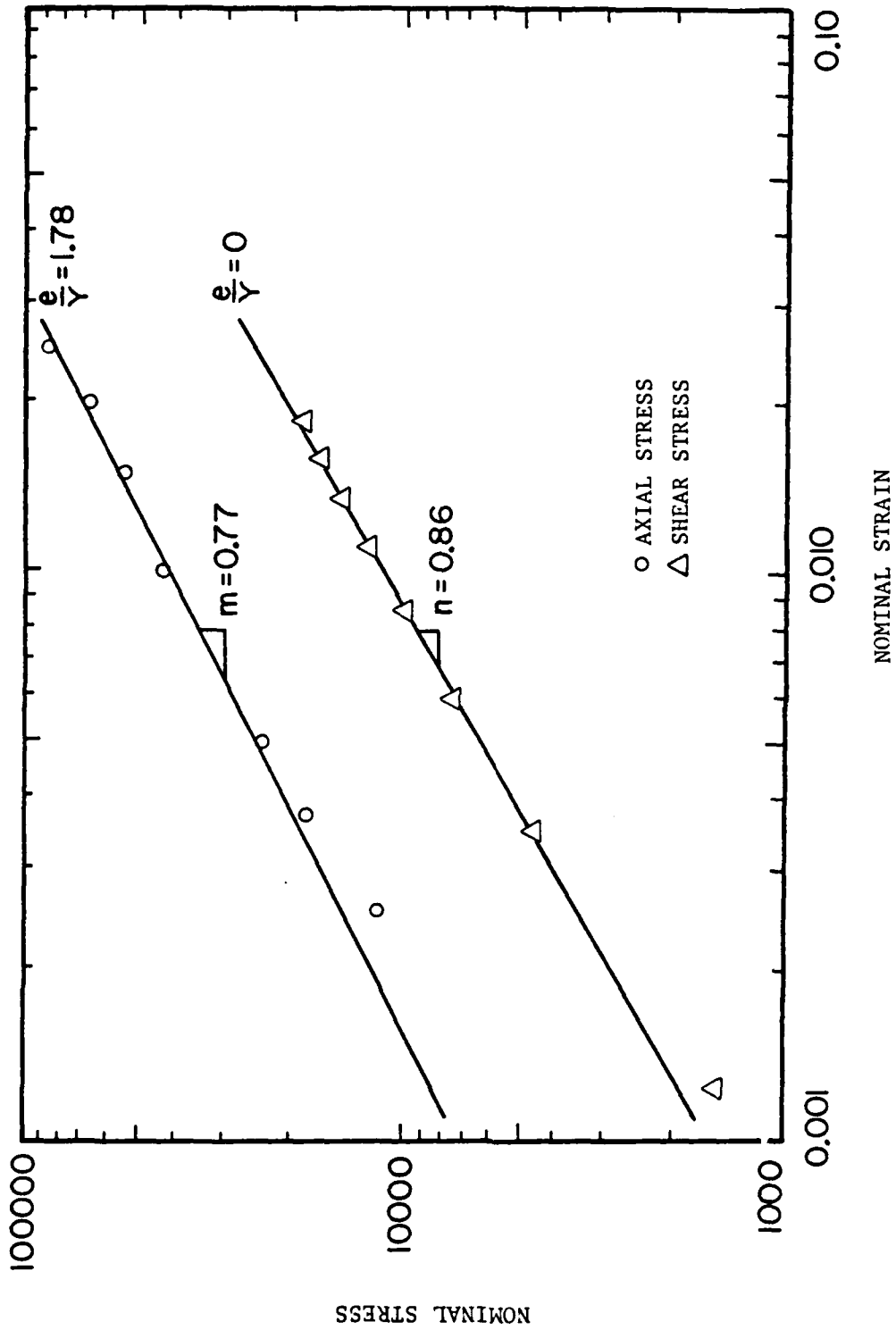


Figure 5. Logarithmic plots of stress-strain data from Figures 3 and 4 showing power law behavior.

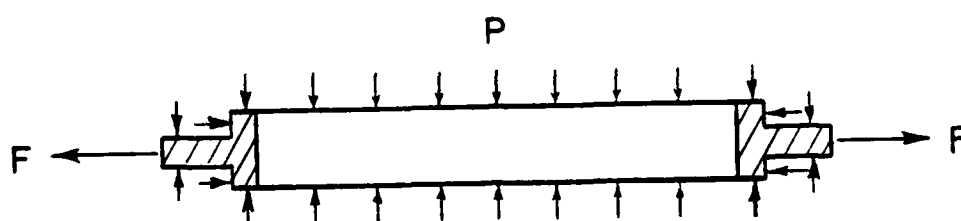


Figure 6. Particle-filled elastomer under pressure and axial loading.

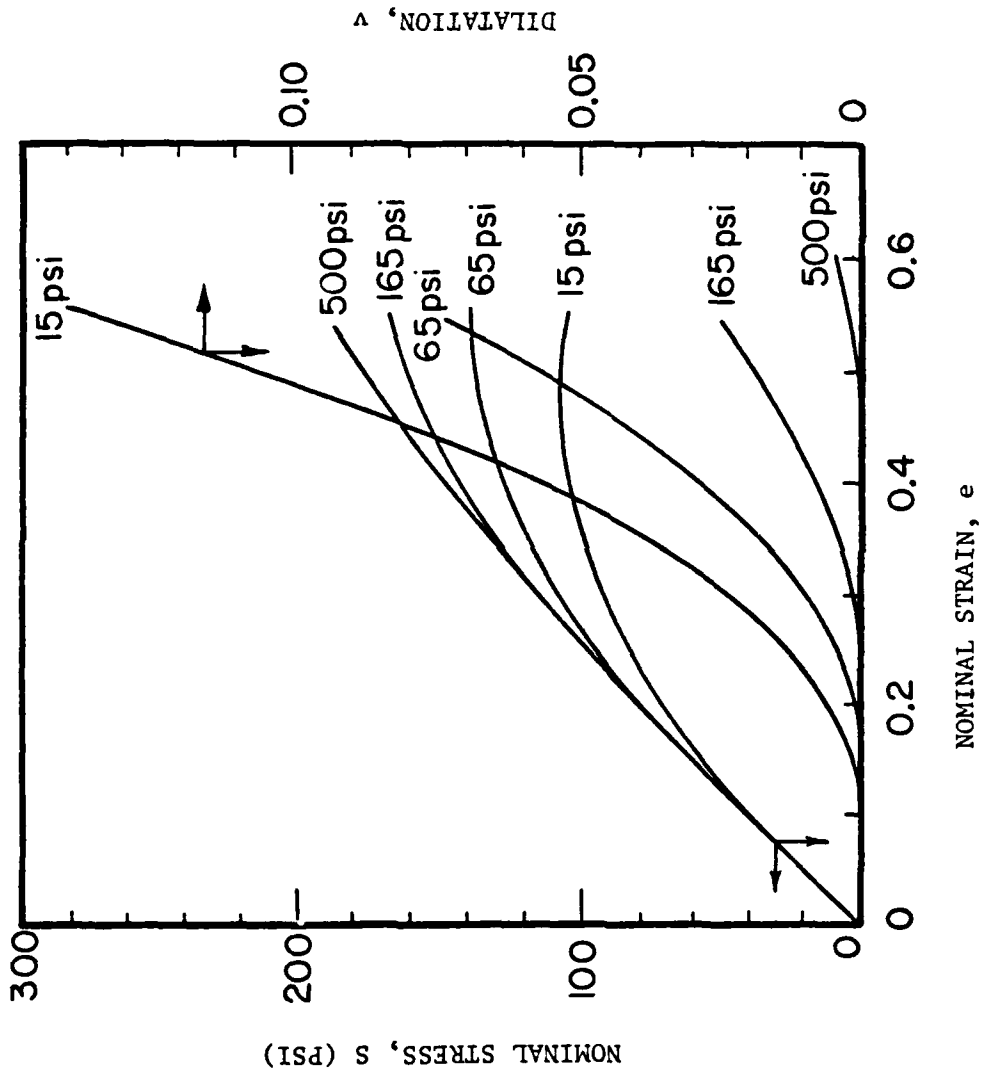


Figure 7. Stress-strain and dilatation-strain behavior of a highly-filled elastomer (65 vol-%) at a series of hydrostatic pressures. After Farris (25).

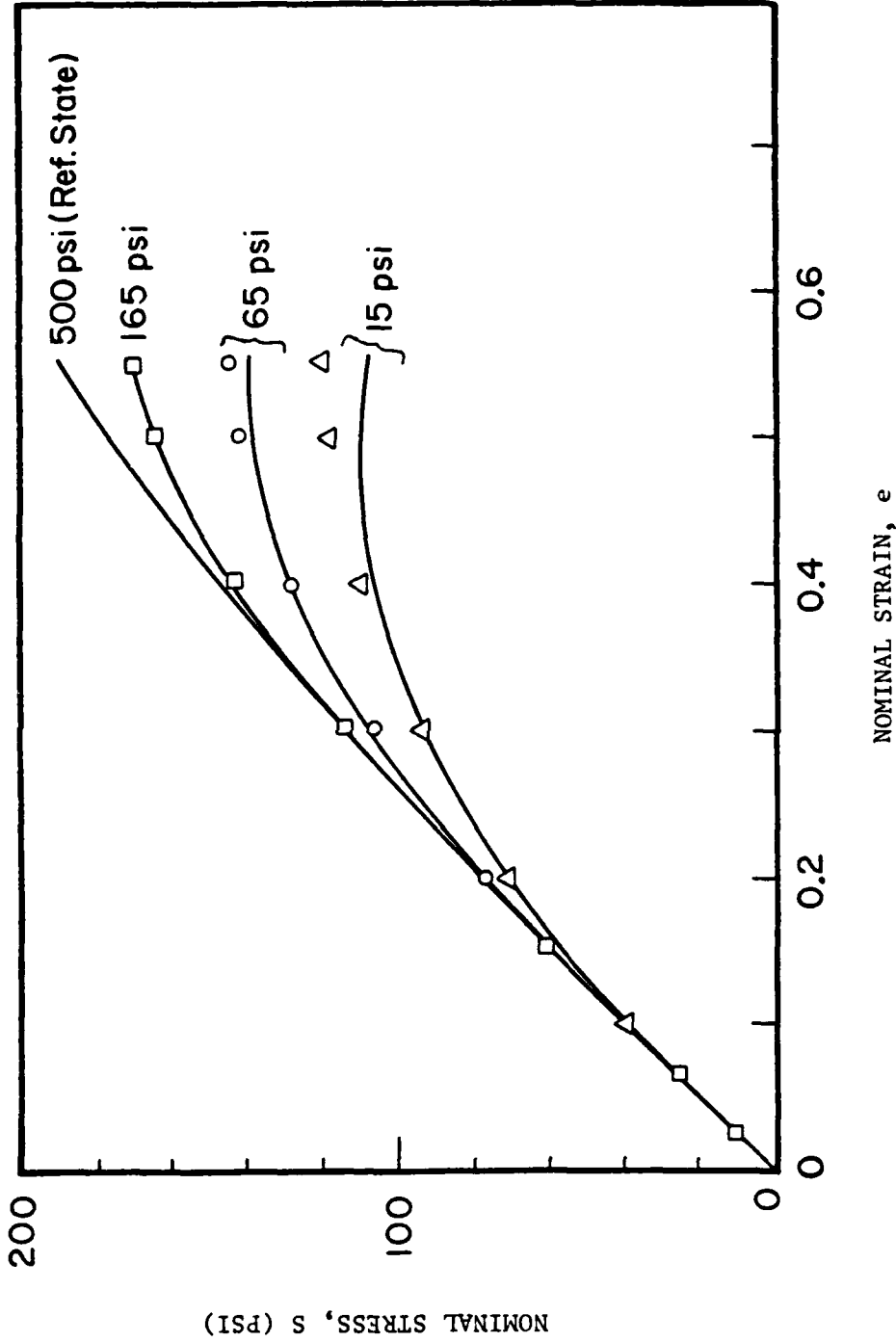


Figure 8. Comparison of calculated (points, Eq. (54)) and measured (lines) stress-strain behavior from data in Figure 7. After Farris (25).

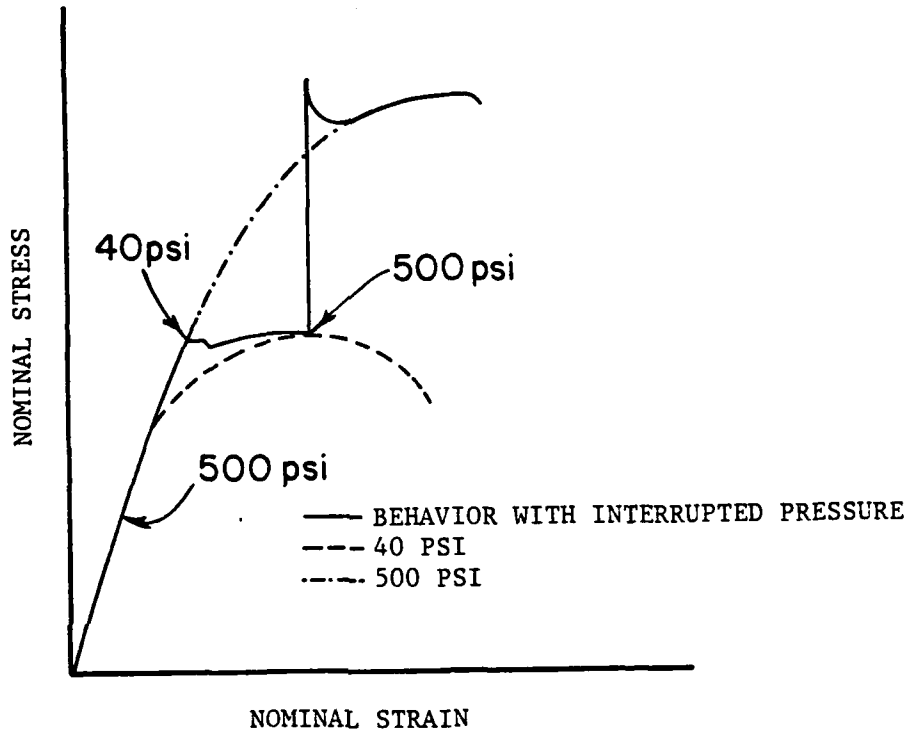


Figure 9. Stress-strain curve for highly-filled elastomer subjected to changes in the pressure level. After Farris (25).

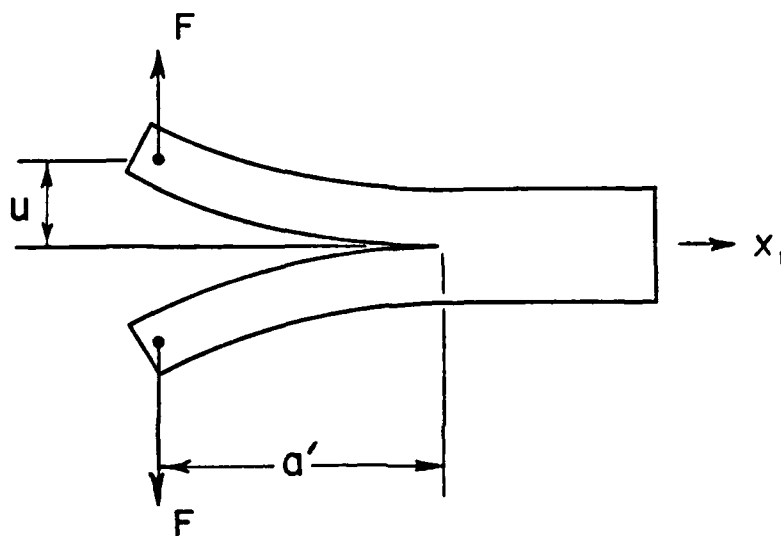


Figure 10. Double cantilevered beam (DCB) for delamination fracture studies.

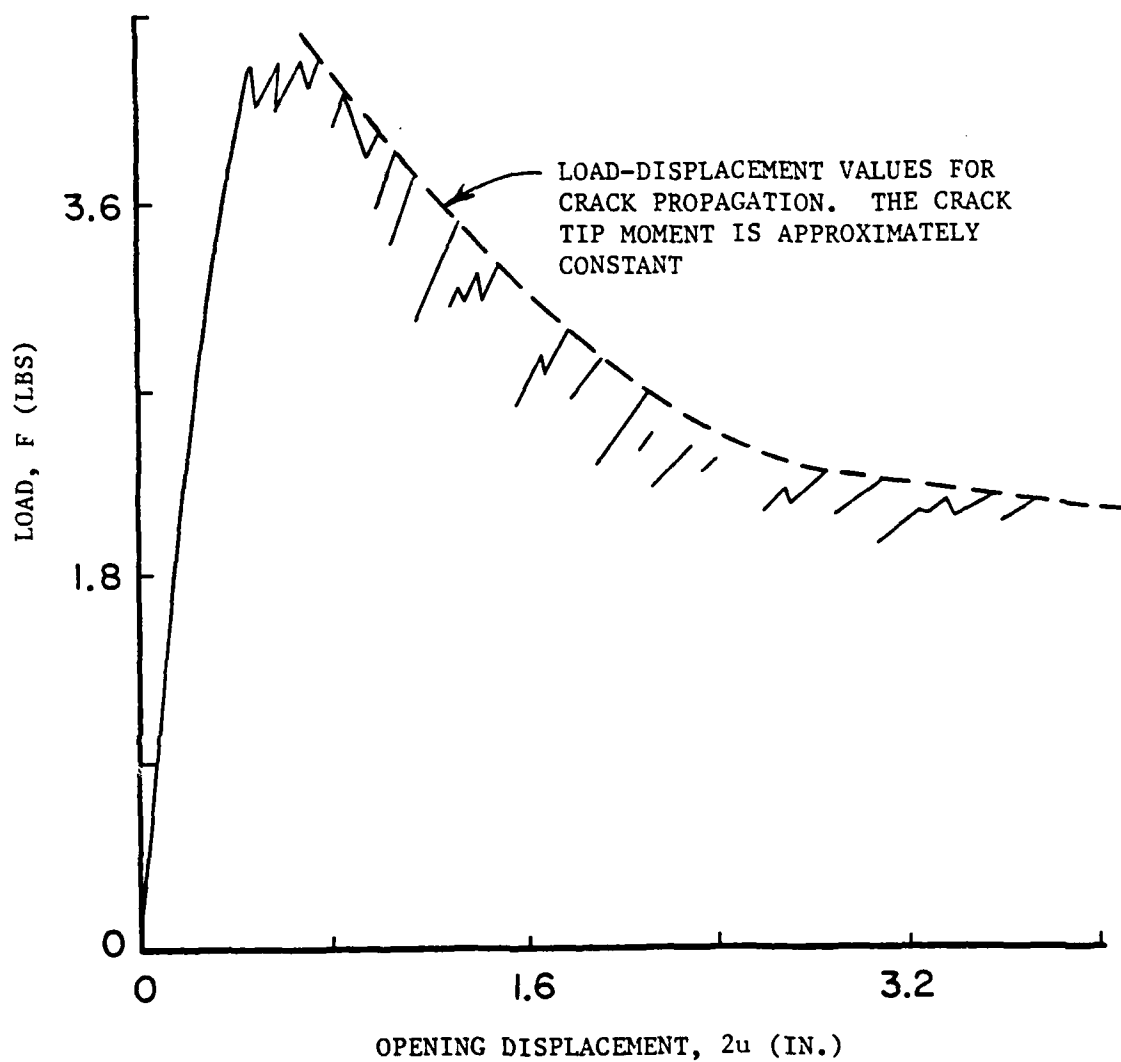


Figure 11. A typical load-displacement record for opening mode loading of a double cantilevered beam with off-axis plies at the center interface. Hercules AS4/3502 graphite/epoxy. After Jordan (26).

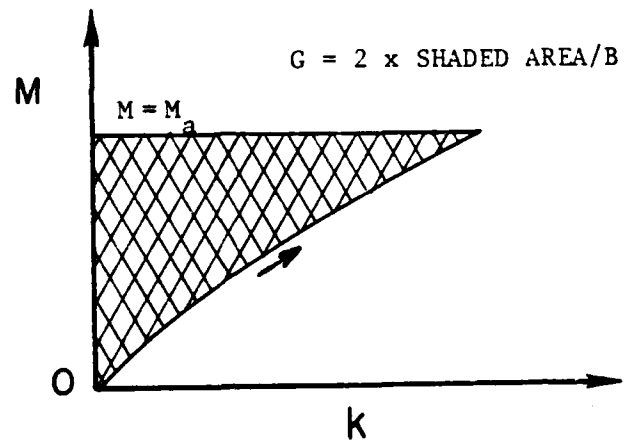


Figure 12. Moment-curvature diagram for loading, showing energy release rate, G .

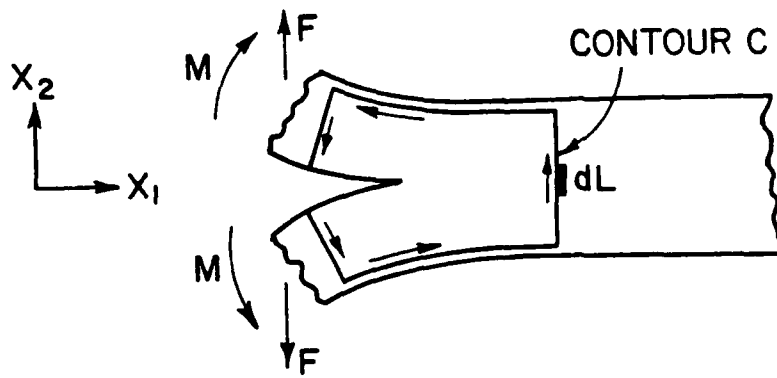


Figure 13. Contour used to evaluate J integral.

Delamination Analysis of Composites with
Distributed Damage using a J integral*

R. A. Schapery
W.M. Jordan
D. P. Goetz

ABSTRACT

The J integral theory for fracture analysis of materials with distributed damage is discussed and then specialized to a form that is useful for analyzing opening-mode delamination crack growth. Tests on double-cantilevered beam specimens of two different graphite/epoxy material systems and three different layups are described and then analyzed.

1. Introduction

Fiber-reinforced plastic laminates may sustain an appreciable amount of microcracking and other types of damage before global structural failure occurs. In order to characterize the resistance to delamination and to predict delamination when there is globally distributed damage such as microcracking, it may be necessary to account for the nonlinear inelastic behavior produced by this distributed damage. In this Section we briefly give some background on the J integral. The theory is then specialized in Section 2 to opening-mode delamination of double-cantilevered beams (DCB) and illustrated in Section 3 using experimental data from tests of two different graphite/epoxy laminates.

A two-dimensional version of the J integral was introduced by Rice [1], and was shown to be especially useful in nonlinear elastic fracture mechanics. Its primary usefulness comes from its path independence and its relationship to the crack tip stress field and work input to the crack tip. Numerous generalizations (including extension to three-dimensions and large strains) and applications have since appeared, such as discussed in a recent book by Kanninen and Popelar [2]. Except for steady-state conditions [3], the properties of the J integral are usually considered to depend on the existence of strain energy potential $W=W(e_{ij})$, where

$$s_{ij} = \partial W / \partial e_{ij} \quad (1)$$

in which s_{ij} and e_{ij} are components of the stress and strain tensors. Schapery extended the J integral to nonlinear viscoelastic materials [4] and further showed that important characteristics of the J integral carry over to other types of inelasticity, including that due to distributed

*Prepared for International Symposium on Composite Materials and Structures, Beijing, China, June 1986.

R.A.S. and D.P.G., Professor, Civil and Aerospace Engineering and Graduate Research Assistant, Mechanical Engineering, respectively, Texas A&M University, College Station, TX 77843. W.M.J., Assistant Professor, Mechanical Engineering, Louisiana Tech University, Ruston, Louisiana 71272.

microcracking and other types of damage [4,5]. These generalizations depend on the existence of a potential which is analogous to strain energy, Eq. (1), but which may be multivalued. Figure 1 illustrates such a potential for uniaxial stressing. The net work input to the sample at any time in the loading or unloading history is the so-called work-potential,

$$W \equiv \int_0^e s \, d e \quad (2)$$

In general, s and W are multivalued functions of e since they depend on whether s is the loading or on the unloading curve. Arguments for the existence of multivalued work potentials in three dimensions which satisfy Eq. (1) were given by Schapery [4,5].

Here we shall assume a work potential exists and use it in a J integral to analyze delamination fracture. For the materials and conditions studied experimentally viscoelastic effects were very small, and these effects are therefore neglected in the theory.

2. J Integral for the DCB Specimen

Figure 2 shows a DCB specimen. In the cases studied here, the beam is a laminate, and applied force F causes the crack to propagate in a plane parallel to the plane of lamination (which is perpendicular to the plane of the page). We assume a' is long enough for the legs to be in plane stress over a significant portion of their length.

The J integral for the DCB specimen is

$$J = \int_C [W dx_2 - (T_1 \frac{\partial u_1}{\partial x_1} + T_2 \frac{\partial u_2}{\partial x_1}) dL] \quad (3)$$

where W is the work-potential per unit volume, T_1 and T_2 are tractions along C , Fig. 3, and u_1 and u_2 are displacements; the indices indicate components in x_1 and x_2 directions. This equation is valid for large strains and rotations as long as we interpret x_1 and x_2 to be coordinates of the undeformed geometry. The integration is counterclockwise along the curve C in Fig. 3, which includes top and bottom beam surfaces and vertical segments. The right vertical segment is taken far enough from the crack tip that the material is unstressed, and thus gives no contribution. Assuming small strains and that the left segment is close enough to the crack tip that we can use small rotation beam theory (but far enough to the left of the tip for plane stress conditions to apply) yields,

$$J = \frac{2}{B} \int_0^M k(M') dM' - 2 \frac{F}{B} \frac{du_2}{dx_1} \quad (4)$$

where M and du_2/dx_1 are the moment and slope, respectively, at the left vertical segment; B is the beam width. Integrate $k = d^2u_2/dx_1^2$ to the tip (assuming plane stress) to obtain the slope, use $dM = F dx_1$ and Eq. (4) reduces to

$$J = \frac{2}{B} \int_0^{M_a} k(M) dM \quad (5)$$

where M_a is the crack tip moment; this is the same result derived by Rice [1] for a split beam under pure end moments M_a . It is seen that the result is independent of the location of the left integration segment and, in fact, is that in Eq. (4) when the segment is located at the crack tip (where $du_2/dx_1 = 0$). It should be mentioned, however, to obtain this path independence (i.e. derive Eq. (5) from (4)) it was necessary to assume if $k(M)$ is multivalued (similar to the s - e curve in Fig. 1) that the unloading curve is the same for all left vertical segments used. This latter

condition will be met for all material (to the left of the current tip) which had experienced the same maximum moment when the crack tip passed by. Inasmuch as the experimental results discussed later indicate the maximum moment is constant (and recognizing that the moment decays with distance from the tip) this condition is met all of the way to the location of the initial crack tip. To the left of the initial tip the maximum moment is less than M_a and one finds J depends on the location of the left segment. This path dependence in beam theory is fully consistent with that predicted from the exact J integral for a continuum with variable damage in the regions of unloading [4].

Strictly speaking one should consider the effect of the three-dimensional state of stress around the crack tip in developing the J integral for the DCB specimen. If indeed one does this starting with the theory in [4], one still arrives at Eq. (5) if the maximum amount of damage is essentially that defined by the beam theory and the slope is adequately predicted by plane stress theory. Weatherby [6] studied this problem using the finite element method for two dimensional deformation of a highly inelastic isotropic beam and found that Eq. (5) is an excellent approximation.

Finally, we observe that for a delamination propagating at a constant tip moment in a long laminate which is homogeneous in the x_1 direction in its initial state, the state of stress and strain in the neighborhood of the tip is constant in time if effects of shear force changes are neglected. This is a type of "self-similar" growth and therefore J is the work input to the crack tip [4] (per unit of new area projected onto the delamination plane).

3. Experimental Study of DCB Specimens

Materials and Test Procedure: Two commercially available graphite/epoxy composites were tested: T6T145/F155 (Hexcel Corporation) and AS4/3502 (Hercules, Incorporated). The epoxy in the former system is toughened with 6 vol. % rubber particles. Several layups were tested as reported by Jordan [7]. Here we report on four different layups with some of the data coming from [7], but most data are from more recent tests.

Prepreg was used to make plates which were cured in the Texas A&M University air-cavity press using the manufacturer's recommended temperature cycle. A thin 3.5 cm wide teflon strip was inserted in the midplane along one edge of each plate during the layup step in order to provide a 3.5 cm long starter crack in the beams cut from the plates; each beam was approximately 2.5 cm wide by 30 cm long. Those layups with off-axis fiber orientations are listed in Table I. Besides these laminates, unidirectional beams with 0° fiber orientation (fibers parallel to the beam axis) for both systems were tested.

Table I
Laminates with Off-axis Fibers

Laminate Designation	Material System	Layup (fiber orientations)	
A	T6T145/F155	[$\pm 45/0(8)/\mp 45(2)/0(8)/\pm 45$]	(24 plies)
B	T6T145/F155	[$\pm 45/\mp 45(2)/\mp 45(2)/\mp 45(2)/\pm 45$]	(16 plies)
C	AS4/3502	[$\pm 45/0(4)/\mp 45(2)/0(4)/\pm 45$]	(16 plies)

In all three cases, the delamination crack was in the middle plane of the beam, between a +45 and -45 ply. For A and C layups the beam legs

above and below the delamination are balanced and symmetric in the undamaged state. These designs were used to minimize twist and bending-stretching coupling to simplify specimen analysis in this exploratory investigation.

At least two samples of each laminate were delaminated in stroke control in a servohydraulic test machine. The test was stopped several times and the beam unloaded to measure the moment arm to the crack tip (loaded state) and length of the delamination (unloaded state), and to determine the force-displacement curve with loading and unloading for use in an energy-based data analysis method.

Additional tests were conducted on single cantilevered beams to obtain the moment-curvature relationship for use in the J integral analysis. These beams were made with fiber orientations corresponding to the layup above the middle surface in the beams used for delamination tests. Strain gages were mounted above and below the beam near the clamped end in order to determine the curvature k from the equation $k = \Delta e/t$ where Δe is the difference in strain readings on the top and bottom surfaces and t is the beam thickness. The beam support at the clamped end was mounted on bearings to provide free axial movement. In these tests and the delamination tests, the external load was applied vertically through bearing-supported pins.

Discussion of Results: Figures 4 and 5 show the force-displacement diagram for two layups in Table 1. Figure 6 shows results from one of the cantilevered beam tests used to obtain the moment-curvature relationship; specimen type B exhibited the most hysteresis. The maximum moment is the crack-tip value determined from the delamination test. According to Eq. (5), J is the area to the left of the loading curve multiplied by $2/B$. Table 2 summarizes the results. Two numbers are given in most cases, each coming from different specimens.

Table 2
Summary of Results on Fracture Toughness
(in J/m^2)

Laminate Designation	J_C (Eq. (5))	J_a (Eq. (5))	G_C (area)	G_C (stiffness [8])
A	615/510	-	601/557	588
B	522	-	725/725	1333
C	538/525	389/380	440/434	383 (arrest value)

The values in the column in Table 2 labeled G_C (area) were obtained by determining the area between successive loading-crack growth-unloading curves (as in Figs 4 and 5). Assuming the specimens are linearly or nonlinearly elastic, this area divided by the new crack surface area is the G_C value required for propagation. The last column is based on the method described by Devitt et al. [8]. It uses load-deflection-crack length data to obtain G_C ; it is based on the assumptions of linear elastic behavior and no midplane strain, but it allows for large rotations. (The beam rotation at the load-point was as high as 40° in layup C; only for layup A was the geometric nonlinearity negligible.) It should be added that all three methods used to develop the values in Table 2 allow for geometric nonlinearities. Material nonlinearities and midplane strains (due here to nonlinearity) are not neglected in the methods used except for that in [8].

For the specimen type C, delamination occurred usually in distinct

steps, as illustrated in Fig. 5. When growth initiated there was a significant and sudden jump in crack length; the loads used in data analysis at each pair of initiation and arrest points are connected by dashed lines. The corresponding moments were used with moment-curvature results to predict J_c (initiation) and J_a (arrest) values. Specimen types A and B delaminated quite smoothly in most cases.

The moment at which propagation occurred was essentially constant for each specimen with the variation being no larger than $\pm 5\%$ from the average. Once or twice during the delamination test of most beams an exceptionally high or small moment was obtained, but these values were not used in calculating the averages in Table 2. (These unusual values did not necessarily occur at either the shortest or longest cracks.) The arrest moment in specimen type C exhibited scatter similar to that for initiation moments.

It is of interest to compare the fracture toughness values in Table 2 with those for the same systems but with all 0° fiber angles. Jordan found that for the Hexcel system G_c varied from 400 to 650 J/m^2 and for the Hercules system G_c varied from 180 to 200 J/m^2 . The former values are consistent with the J_c values in Table 2 (specimen types A and B), whereas the latter values are less than one-half those reported in Table 2 (specimen type C). These low values are consistent with observation of fracture surface roughness, in that the surface of the 0° fiber specimen was very smooth, whereas many microcracks running parallel to fibers could be seen on C type specimens.

The B specimens do not have any 0° fibers, and therefore the effect of distributed damage in the legs should be the largest. It is believed the high G_c values reported for this layup using the deflection-based methods, compared to J_c , reflect this fact. For example, the area method gives a G_c which includes the work of both distributed damage and delamination.

4. Conclusions

A relatively simple expression, Eq. (5), was developed for determining the J integral. Only the work of bending was considered for the beam near the delamination tip; however, the analysis could be readily generalized to allow for shear and axial deformation work when appropriate. The preliminary assessment of the approach using double-cantilevered beam specimens is very encouraging. As predicted by the theory, it was found that the delamination propagated at essentially a constant crack-tip moment. Also, for one material system it yielded fracture toughness values which are essentially the same for three different layups. In contrast, the other deflection-based methods typically yielded higher toughness values when distributed damage was significant.

Acknowledgements

This research was sponsored by the U.S. Air Force Office of Scientific Research, Office of Aerospace Research. The authors are grateful to Messrs. B.C. Harbert and R.E. Jones, Jr. for their help on portions of the experimental work.

References

- [1] Rice, J., "A Path Independent Integral and the Approximate Analysis of Strain Concentration by Notches and Cracks," *J. Appl. Mech.*, Vol. 35, 1968, pp. 379-386.
- [2] Kanninen, M.F., and Popelar, C.H., Advanced Fracture Mechanics, Oxford Univ. Press, New York, 1985.
- [3] Budiansky, B., Hutchinson, J.W., and Lambropoulos, J.C., "Continuum Theory of Dilatant Transformation Toughening in Ceramics," *Int. J. Solids Structures*, Vol. 19, 1983, pp. 337-355.

- [4] Schapery, R.A., "Correspondence Principles and a Generalized J Integral for Large Deformation and Fracture Analysis of Viscoelastic Media," *Int. J. Fracture*, Vol. 25, 1984, pp. 195-223.
- [5] Schapery, R.A., "Deformation and Fracture Characterization of Inelastic Composite Materials Using Potentials," Texas A&M Report No. MM-5034-85-22, Dec. 1985.
- [6] Weatherby, J.R., "Finite Element Analysis of Crack Growth in Inelastic Media", Ph.D. Dissertation, Mechanical Engineering Dept., Texas A&M Univ., May 1986.
- [7] Jordan, W.M., "The Effect of Resin Toughness on the Delamination Fracture Behavior of Graphite/Epoxy Composites," Ph.D. Dissertation, Mechanical Engineering Dept., Texas A&M Univ., Dec. 1985.
- [8] Devitt, D.F., Schapery, R.A., and Bradley, W.L., "A Method for Determining the Mode I Delamination Fracture Toughness of Elastic and Viscoelastic Composite Materials," *J. Composite Materials*, vol. 14, 1980, pp. 270-285.

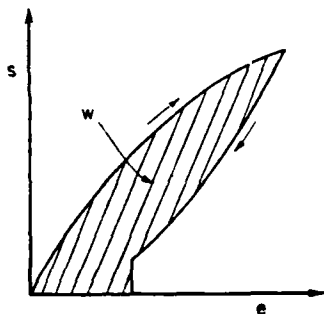


Figure 1. Uniaxial stress-strain curve for material with increasing damage during loading and constant damage during unloading.

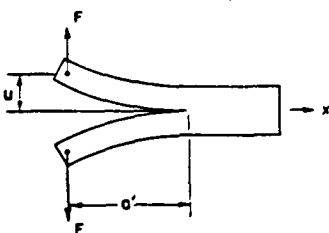


Figure 2. Double-cantilevered beam (DCB) for delamination fracture studies.

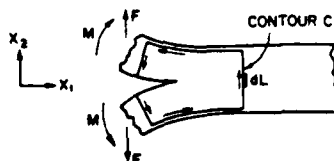


Figure 3. Contour used to evaluate J integral

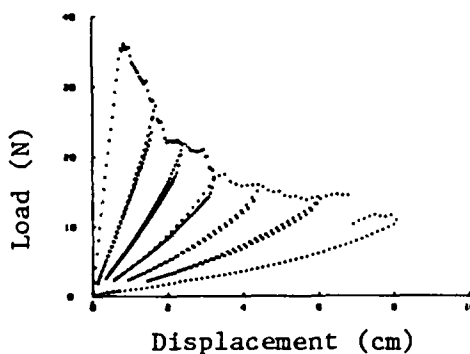


Figure 4. Load vs. displacement ($2u$) for type B specimen.

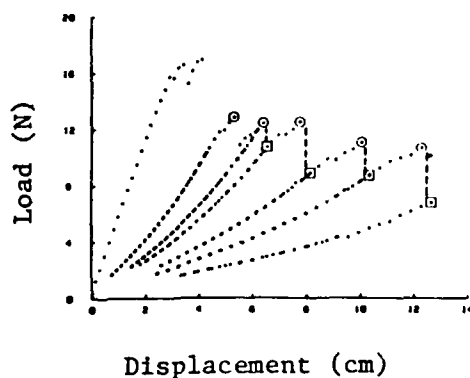


Figure 5. Load vs. displacement ($2u$) for type C specimen.

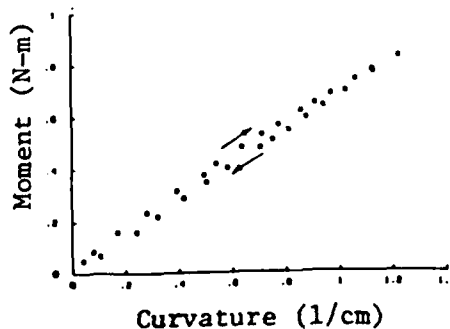


Figure 6. Moment-curvature for type B specimen

Finite Element Analysis of Crack Growth in Inelastic Media^{1,2}

J. R. Weatherby
Sandia National Laboratories, Division 1521
R. A. Schapery
Texas A&M University

In most materials, macrocrack extension is accompanied by inelastic phenomena (such as microcracking or plastic deformation) throughout a region surrounding the crack tip. Immediately ahead of the crack tip, strain localization occurs in a small volume of heavily damaged material referred to as the failure zone or fracture process zone. In this study, the failure zone and the surrounding zone of inelastic material are treated as two distinct regions. The failure zone is assumed to be thin relative to its length and is represented in a two-dimensional finite element model as tractions which act across the crack faces near the tip. An opening mode of crack tip deformation is assumed. The normal traction at any point on the crack surface in the failure zone is specified as a decreasing function of the crack opening displacement which vanishes after a critical value of displacement is reached. Two different rate-independent, inelastic continuum characterizations based on multivalued work-potentials are used; one models metal plasticity and another represents microcracking in brittle materials. Both constitutive models allow for the definition of

¹This abstract was prepared for publication in the Proceedings of the 10th U.S. National Congress of Applied Mechanics, June 1986.

²Based on the first author's Ph.D. dissertation, "Finite Element Analysis of Crack Growth in Inelastic Media," Mechanical Engineering, Texas A&M University, (May, 1986).

a generalized J-integral developed by Schapery^{3,4}, which has the same value for most paths around the crack tip for realistic distributions of plasticity or damage in the material surrounding a stationary or propagating crack. This path independence and the equivalence between J and the work input to the last ligament of material in the failure zone are verified numerically in a transient crack growth problem; both initiation and propagation are studied under conditions of small-scale inelasticity. Steady-state crack growth is studied in two different specimen geometries. Simplified J-integral analyses are used to estimate the work input to the failure zone for these steady-state problems. The J-integral estimations are compared with finite element results to determine the accuracy of the simplified analyses.

³R.A. Schapery, "Correspondence Principles and a Generalized J-Integral for Large Deformation and Fracture Analysis of Viscoelastic Media," International Journal of Fracture, 25 (1984) 195.

⁴R.A. Schapery, "Deformation and Fracture Characterization of Inelastic Composite Materials Using Potentials," Texas A&M Report No. 5034-85-22, 1985.

END

1-87

DTIC